Graphical Abstract

Vent communities of
Bathymodiolus azoricus
Lucky Strike vent field
MAR, 1700 m

Experimental disturbance by removing faunal assemblages

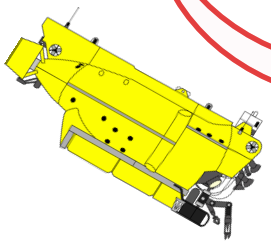

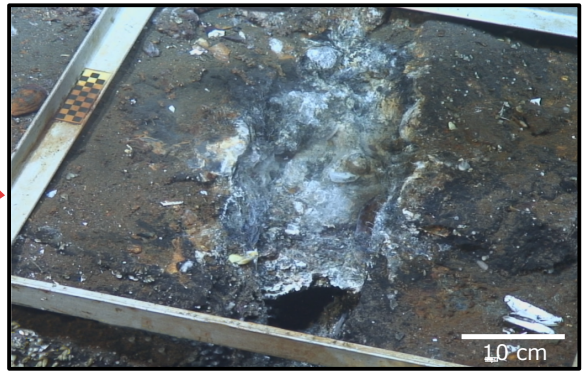

High recovery in taxonomic richness

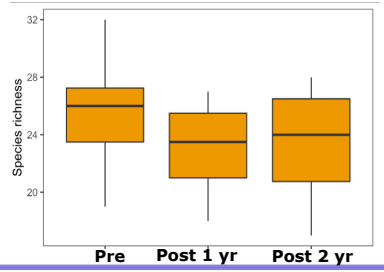

Incomplete recovery in faunal density

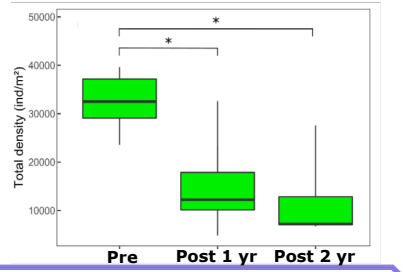

Assess the recovery and follow the recolonisation process within 2 years

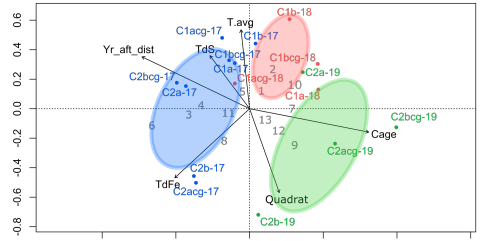

Significant difference in faunal composition in **pre-disturbed**, **1** and **2** years after disturbance

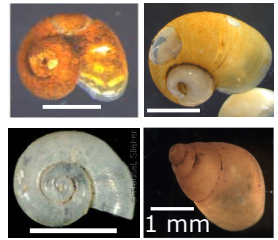

Gastropod species pioneer colonists

Recovery of hydrothermal vent communities in response to an induced disturbance at the Lucky Strike vent field (Mid-Atlantic Ridge)

Marticorena J.[1]*, Matabos M.[1]*, Ramirez-Llodra E.[2,3], Cathalot, C.[4], Laes-Huon, A.[5], Leroux R.[6], Hourdez S. [7], Donval J-P. [4], Sarrazin J.[1]*

[1] *Ifremer, REM/EEP, F-29280 Plouzané, France*

[2] *Norwegian Institute for Water Research, Gaustadalleen 21, 0349 Oslo, Norway*

[3] *REV Ocean, Oksenøyveien 10, 1366 Lysaker, Norway*

[4] *Ifremer, REM/GM/LCG, F-29280 Plouzané, France*

[5] *Ifremer, REM/RDT/LDCM, F-29280 Plouzané, France*

[6] *Research Centre for Watershed-Aquatic Ecosystem Interactions, Université du Québec à Trois-Rivières, Trois-Rivières, QC G9A 5H7, Canada*

[7] *Observatoire Océanologique de Banyuls-sur-Mer, UMR 8222 CNRS-SU, 1 avenue Pierre Fabre, 66650, Banyuls-sur-Mer, France.*

*Corresponding authors : Julien Marticorena (julienmarticorena@gmail.fr), Marjolaine Matabos (Marjolaine.matabos@ifremer.fr), Jozée Sarrazin (Jozee.sarrazin@ifremer.fr),

Abstract

So far, the natural recovery of vent communities at large scales has only been evaluated at fast spreading centres, by monitoring faunal recolonisation after volcanic eruptions. However, at slow spreading ridges, opportunities to observe natural disturbances are rare, the overall hydrothermal system being more stable. In this study, we implemented a novel experimental approach by inducing a small-scale disturbance to assess the recovery potential of vent communities along the slow-spreading northern Mid-Atlantic Ridge (nMAR). We followed the recovery patterns of thirteen Bathymodiolus azoricus mussel assemblages colonising an active vent edifice at the Lucky Strike vent field, in relation to environmental conditions and assessed the role of biotic interactions in recolonisation dynamics. Within 2 years after the disturbance, almost all taxonomic richness had recovered, with the exception of a few low occurrence species. However, we observed only a partial recovery of faunal densities and a major change in faunal composition characterised by an increase in abundance of gastropod species, which are hypothesised to be the pioneer colonists of these habitats. Although not significant, our results suggest a potential role of mobile predators in early-colonisation stages. A model of post-disturbance succession for nMAR vent communities from habitat opening to climax assemblages is proposed, also highlighting numerous knowledge gaps. This type of experimental approach, combined with dispersal and connectivity analyses, will contribute to fully assess the resilience of active vent communities after a major disturbance, especially along slow spreading centres targeted for seafloor massive sulphide extraction.

Key words: Hydrothermal vent; *Bathymodiolus azoricus*; Disturbance; Colonisation; Recovery; Deep-sea mining; Ecological succession; Benthic ecology; Mid-Atlantic Ridge

1. Introduction

Deep-sea hydrothermal vents are mainly distributed along mid-ocean ridges and back-arc basins. Vent communities are considered as productivity hotspots with a high level of endemic fauna (Tunnicliffe, 1991) that thrives mainly on chemoautotrophic primary production (Childress and Fisher, 1992). Faunal assemblages are often dominated by symbiotic foundation species such as siboglinid tubeworms, mytilid mussels, large provannid gastropods or alvinocaridid shrimps, which promote local diversity by providing 3D structures and enhancing habitat heterogeneity (Dreyer et al., 2005; Govenar and Fisher, 2007). At the edifice scale, faunal distribution consists in a mosaic of assemblages mainly influenced by environmental conditions and patchiness of fluid emissions (Sarrazin et al., 1997; Sarrazin and Juniper, 1999; Luther et al., 2001; Gollner et al., 2010; Marsh et al., 2012; Husson et al. 2017). Indeed, species colonise the mixing gradient depending on their physiological tolerance to environmental conditions, nutritional requirements and biotic interactions (e.g. predation, facilitation; Levesque et al. 2003, Mullineaux et al. 2003, Sancho et al. 2005). Biotic interactions were suggested to prevail in high diffuse-flow areas where the resources are not limited, while facilitation will predominate in habitats with lower fluid input (Mullineaux et al. 2003). As observed in coastal hard substrate communities, mosaics are highly dynamic and patche's size and boundaries amongst the patched may change through time (Connell and Keough, 1985). At large spatial scale, the patchiness of vent habitat results in a network of metacommunities and population connectivity is insured by dispersal of planktonic larvae (Mullineaux et al., 2018).

Hydrothermal vents are naturally subject to stochastic major disturbance such as volcanic eruptions that may eradicate faunal assemblages at the vent-field scale. On the other hand, since the first discovery of hydrothermal vents and associated seafloor massive sulphide (SMS) deposits, more than 40 years ago, the interest of mining companies for commercial exploitation of their high metal content has been increasing (Corliss et al., 1979; Spiess et al., 1980; Van Dover, 2011). These industrial activitiy has not yet started, but it is predicted that they may induce different levels of impacts (Boschen et al., 2013; Cuvelier et al., 2018; Orcutt et al., 2020), including physical destruction of habitats and the complete eradication of their faunal communities within the mining site (Van Dover 2007). The creation of a sediment plume may also affect different biological processes, such as reproduction, dispersal, mobility

and feeding strategies at larger scale (Van Dover, 2010; Boschen et al., 2013; Gollner et al., 2017; Suzuki et al., 2018; Washburn et al., 2019). However, there are still many uncertainties about community resilience, and the time-scale needed for a possible recovery of the impacted ecosystems (Cuvelier et al., 2018).

Disturbance in mosaic habitats such as active vents may play an important role in initiating, maintaining or enlarging patches within established assemblages (Sousa 1985; Denny 1987). The fundamental question of recolonisation and recovery of vent assemblages after a disturbance can be studied in a metacommunity framework, using a patch dynamics approach in which the colonisation and persistence of impacted area is highly dependent on dispersal across vent fields and local disturbance regimes (Leibold et al., 2004; Mullineaux et al., 2018). At local scale, the settlement of post-larvae is influenced by environmental conditions and habitat suitability and recolonisation dynamics are also dependent on biotic interactions that may induce facilitation or competitive exclusion (Mullineaux et al., 2003; Sancho et al., 2005). Understanding processes acting at small scales are paramount in evaluating mechanisms controlling successional dynamics after recolonisation by species from afar.

At active vents, the few examples of recovery are based on studies linked to large-scale natural disturbances caused by volcanic and tectonic activities (Butterfield et al., 1997; Tunnicliffe et al., 1997; Shank et al., 1998; Marcus et al., 2009; Gollner et al., 2015a). The frequency of such disturbances is highly variable among vent systems, depending on their geological settings. At fast-spreading ridges, where vent sites are separated by a few kilometers, volcanic eruptions occurs with time intervals of a decade (Tolstoy et al. 2006) and macrofaunal communities show a fairly good recovery of diversity and densities within few years following the various eruptions (Tunnicliffe et al. 1997; Shank et al. 1998; Marcus et al. 2009; Gollner et al. 2015a, 2017, 2020). However, differences in the sampling methodology between these studies (e.g. some used visual surveys while others sampled faunal assemblages) and the faunal compartment considered lead to differences in the estimation of recovery rates. Moreover, little information about the pre-disturbed baseline communities was available, making the comparison with post-disturbance communities difficult. Differences in community composition after re-colonisation were also observed (Mullineaux et al., 2020, 2012) and the prolonged monitoring of diversity showed that community composition was still changing ten years after the disturbance, suggesting that the disturbed

assemblages did not reach a climax stage during this time period (Mullineaux et al., 2020). Conversely, at slow spreading ridges, vent sites are separated by hundreds of kilometers (Beaulieu et al., 2015) and opportunities to observe natural disturbances are rare. Therefore, assessing the recovery ability of communities requires the use of alternative indirect approaches. One way is to use population connectivity data to estimate the recolonisation potential of key species, and thus infer vent community recovery rates (Baco et al., 2016; Breusing et al., 2016) as it was done by Suzuki et al. (2018). Their dispersal network analysis on species from 131 vent fields of the western Pacific Ocean estimated that a full recovery to original communities would take from 6 to 130 years. The slow recovery rate estimated in comparison to fast-spreading centers may notably be due in part to differences in topography that may reduce horizontal dispersal and connectivity (Mullineaux et al. 2018). However, this approach based on dispersal ability does not take into account the local factors influencing faunal establishment and many uncertainties remain regarding the role of biotic and abiotic conditions in recolonisation dynamics and ecological succession once the larvae reach the disturbed area.

In the present study, we provide an early evaluation of the recovery potential of active vent communities to a small-scale (< 1 m^2) disturbance experiment initiated in 2017 on the Lucky Strike (LS) vent field, northern Mid-Atlantic Ridge (nMAR). After removing the fauna, we followed during 2 years the recolonisation dynamics of *Bathymodiolus azoricus* mussel assemblages and their habitats on a series of experimental quadrats. This experimental setting allowed us to describe the pre-disturbed structure of vent communities on the Montségur edifice (LS) and to monitor the recolonisation of benthic communities after the disturbance. The main objective of this work is to identify the role of biotic and abiotic conditions on recolonisation dynamics at the edifice scale, through the use of cages and measurements of environmental conditions. We expected that microbial communities would first colonise the bare substratum, followed by grazers (including several species of gastropods) that may feed on microbial mats. The engineer species *B. azoricus* would take more time to fully occupy the space, its presence facilitating the establishment of associated taxa and contributing to increasing diversity. We anticipated that mobile predators (e.g. shrimps, crabs or fishes) would play a major role in patch colonisation, influencing the first step of recovery. Although the scale and target of this experiment strongly differ from large-scale disturbance, our results

provide fundamental knowledge on recolonisation patterns of active hydrothermal vent habitats at the edifice scale.

2. Material and methods

2.1. Study site

The Lucky Strike (LS) vent field is a basalt-hosted vent field situated close to the Azores Triple Junction on the northern part of the Mid Atlantic Ridge (MAR) (Langmuir et al., 1997) (Fig. 1A). LS contains over twenty active hydrothermal edifices distributed around a circular fossilised lava lake at an average depth of 1700 m (Ondreas et al., 2009). Montségur is a small active sulphide edifice that extends over a surface of 24 m x 16 m. It is located on a flat hydrothermal slab at the south-east of LS (Fig. 1B). At least seven black smokers have been identified on the edifice, in addition to the extensive diffuse low-temperature discharges through cracks at its base and on its flanks (Barreyre et al., 2014). Montségur is covered by dense mussel assemblages of the engineer species *Bathymodiolus azoricus*. Vent faunal communities inhabiting diffuse flow areas on and around the edifice are characterised by high-density populations of gastropods (*Protolira valvatoides, Lepetodrilus atlanticus, Pseudorimula midatlantica*), polychaetes (*Branchipolynoe seepensis, Amphisamytha lutzi*) and shrimps (*Mirocaris fortunata*) (Sarrazin et al. 2020).

2.2. Experimental setup

In July 2017, an experimental setup was deployed during the Momarsat cruise on board the R/V "*Pourquoi pas ?*" using the Remotely Operated Vehicle (ROV) *Victor6000*. Thirteen stainless steel quadrats (50 x 50 cm), equipped with pyramidal structures on top, were installed over *Bathymodiolus azoricus* assemblages (Fig. 2), on the steep walls of the Montségur edifice or in cracks at its base (Fig. 1C), to account for spatial variability of vent assemblages. Eight of them, named "experimental quadrats", were devoted to the study of recolonisation processes following faunal clearance after 1 (C1) and 2 (C2) years (August 2018 and June 2019 respectively). Replicate samples for each year were denoted as "a" or "b" (Fig. 1C). In addition to the experimental quadrats, five "reference" quadrats (R) were deployed and sampled in 2017 (R0a, R0b), 2018 (R1) and 2019 (R2, R2cg) to characterise the natural dynamics of faunal communities on Montségur throughout the experiment. The role of large mobile predators (crabs, shrimp or fish) on local recolonisation was examined by covering

some of the pyramidal structures with a 1 cm plastic mesh. These specific quadrats were denoted as “cg'' for caged (Fig. 2C). This experimental design is summarised in Figure 3.

2.3. Environmental characterisation

Temperature and key chemical parameters were assessed from *in situ* measurements on all quadrats before and after faunal sampling and this, for each year of the study (2017 to 2019). Our objectives were to identify the spatial and temporal variability of these factors and evaluate their role in the recolonisation processes. The *in situ* chemical analysers CHEMINI (Vuillemin et al., 2009) were used on three replicate points in each quadrat to measure dissolved concentration of total sulphides [TdS : $H_2S+HS^-+S_2$] and total dissolved iron [TdFe : Fe (II)]. To complete the chemical characterisation, water samples were collected with the PEPITO water sampler at each quadrat prior to faunal sampling (Sarradin et al., 2009). Oxygen concentrations were measured using an Aanderaa optode probe (Tengberg et al. 2006) connected to the outlet of the PEPITO sampler. Methane [CH_4], was analysed back in the laboratory by GC-FID and HID (Donval et al. 2008). In addition to this one-time yearly characterisation, temperature was monitored every 2 hours over the deployment period using two iButtons™ probes attached to each quadrat and deployed directly on the mussel assemblages with a measurement resolution of 0.5 °C.

2.4. Faunal sampling and identification

During the Momarsat 2017 cruise, eight experimental quadrats -noted “C”- were cleared of their fauna using both the suction sampler and the claw of the ROV *Victor6000* mechanical arm (Fig. 2A, 2B). The same year, R0a and R0b reference quadrats were also sampled, leading to a total of 10 quadrats used to describe the pre-disturbed vent community of Montségur (Fig. 3). During Momarsat 2018, the four experimental quadrats dedicated to the “one-year after disturbance recolonisation study” -noted “C1”- and reference quadrat R1 were sampled (5 quadrats in total; Fig. 3). During the Momarsat 2019 cruise, the four experimental quadrats dedicated to the “two-year after disturbance recolonisation study” noted “C2”-and reference quadrats R2 and R2-cg were sampled (6 quadrats, Fig. 3). The surface area of each quadrat was filmed before and after faunal sampling with the ROV high definition cameras to estimate

the sampled surfaces using imagery analysis (Fig. 2A, 2B). A target with 7 mm checkerboard squares was fixed on each quadrat, providing scaling in the field of view (Fig. 2B).

In this study, fauna will include macrofauna and any meiofauna taxa larger than 250 µm (nematodes, copepods and ostracods). We also include species often considered as megafauna (shrimp, mussels) recovered within the quadrats. The faunal samples were preserved in 96% ethanol. All individuals collected were identified to the lowest possible taxonomic level under a stereomicroscope and counted.

2.5. Population size structure

Size-frequency distributions of the six most dominant species were analysed for each sample of the Montségur edifice. Each individual was measured, using different measurements depending on the species (see details in Table S1). The biggest individuals were measured using a caliper while small individuals were measured on screen to the nearest 0.001 mm, using the Leica Application Suite software. Measurement error was calculated as the maximum difference among 10 measurements of the same individual on 10 specimens comprising a range of all sizes for each species (Table S1). For each assemblage sampled, length-frequency distribution was plotted for the six species. Size class intervals were chosen according to three criteria: i) most size-classes must have at least five individuals; ii) the number of adjacent empty classes must be minimised; and iii) the interval has to be greater than the measurement error (see Jollivet et al. 2000). Size-frequency distributions were compared to a normal distribution using a one-sample Kolmogorov-Smirnov test and differences between the pre-disturbed and post-disturbance communities were identified using a pairwise Kolmogorov-Smirnov test. Non-parametric Wilcoxon-Mann-Whitney tests were performed to identify differences in mean individual size between the pre-disturbed community and the novel one, after the recolonisation processes in each location.

2.6. Data analyses

All analyses were computed in R environment (R Core Team, 2018). Species rarefaction curves were computed for each sample, habitat and year to verify the robustness of the sampling effort and characterise the overall diversity. Local diversity was estimated for each assemblage by computing α-diversity indices such as species richness (S), Shannon entropy (H) and the Pielou's evenness index (J') using the vegan package in R (Oksanen et al., 2019). Contingency

tables were weighted by the sampling surface for each quadrat for comparison purposes. The resulting density data were used for all subsequent analyses.

Environmental conditions – The temperatures measured by the iButtons^{TM} probes were used to characterise each assemblage/quadrat. Four temperature parameters were compiled, including the average (T.avg), minimum (T.min), maximum (T.max) and standard deviation (T.sd). In addition, average concentrations of oxygen (O_2), methane (CH_4), total dissolved iron (TdFe) and sulphides (TdS) as well as standard deviations of TdFe and TdS were used to characterise the spatial variability of abiotic factors among the different Montségur quadrats. A principal component analysis (PCA) was built with all environmental variables (packages FactoMineR and factoextra - Kassambara and Mundt 2019) to identify patterns in environmental conditions among quadrats and determine which variables accounted for most of the observed variance. Finally, Whittaker-Robinson periodograms, programmed in the R package adespatial (Dray et al., 2020) were used to screen for significant periodicities in temperature time series.

Community structure – A canonical redundancy analysis (RDA) was performed on Hellinger-transformed densities and environmental variables retained by a forward selection (vegan package - Oksanen et al. 2019) to evaluate the spatial variability of community composition in relation to abiotic factors in the baseline communities on the Montségur edifice. This allows us to evaluate the representativeness of baseline communities in Montségur in comparison with faunal assemblages already described on other active edifices of the Lucky Strike vent field.

Recovery patterns – Faunal recovery patterns were assessed from experimental quadrats. Differences in faunal composition among quadrats along the recolonisation processes were tested using a non-parametric analysis of similarity (ANOSIM; Anderson 2001). The ANOSIM R value is based on differences in average ranking of dissimilarity indices (i.e. Bray-Curtis dissimilarity matrix) between and within the different predefined groups (here each recovery stage, i.e.: pre-disturbed state, one year and two years after disturbance). A RDA on Hellinger-transformed densities data was also used to identify the role of environmental conditions and biotic interactions (i.e. by testing the cage effect) on the structure of macrofaunal assemblages during the recolonisation processes. A variable named “quadrat” was used to evaluate the independence of the samples from the same quadrat over the years in the explanatory

environmental matrix. Moreover, to test for the effect of time after disturbance, we coded a quantitative variable named “Yr-aft-dist” (i.e. year after disturbance). In this framework, pre-disturbed reference samples were considered as baseline communities at an equilibrium state and thus were coded with a value greater than 2 years. As the age of the natural community is unknown, analyses were run with different values [3 years, 10 years and 100 years] but they all yielded to similar results. Based on previous studies about the temporal stability of these communities (more than 14 years on Eiffel Tower, Cuvelier et al. 2011b) and data about recovery time in other vent system after a major disturbance (4-5 years, Gollner et al. 2017), we considered 10 years as a good compromise to be used for the analysis.

3. Results

3.1. Environmental conditions

Mean temperature among the different quadrats of Montségur varied between 5.2 °C and 9.5 °C (Table 1). R1 and C2a exhibited the highest maximum temperatures (with maximum of 16.1 °C and 22.1 °C respectively), but also higher concentrations in TdFe and CH_4 associated with a more acidic pH (Table 1, Fig. S1).

The two temperature probes separated by ~ 10 cm deployed on each quadrat were used to characterise the spatial variability of abiotic conditions at fine scales. While homogeneous temperatures are observed within some quadrats (e.g. C1a, C1bcg, C2b, C2bcg), others showed a high variability of temperatures in the narrow spatial gradient (few centimetres, e.g. C1b, C2acg); (Fig. S2).

Notable differences in temperature on single quadrats between the two years were observed. C1b, C1acg and C2a quadrats showed a sharp decrease in mean and variability of temperatures at different times during the first year of deployment (Fig. S2). Periodogram analyses carried out on temperature time series revealed significant periods of 12 h for most quadrats. In addition, significant periods of 24 h were also identified on all quadrats except C1acg. Additional periodic signals, possibly harmonics related to the tidal signal, with periods of 36 h and 48 h, were also revealed for C1a, C1acg and C1bcg.

3.2. Pre-disturbed communities

The rarefaction curves built for each pre-disturbed sample of Montségur (Fig. S3) nearly reached an asymptote showing that the sampling effort was sufficient to capture the overall taxonomic diversity of macrofaunal benthic communities of active vent habitats. In total, 43 taxa were identified among a total of 34 158 individuals in the different samples. Most assemblages were characterised by a taxonomic richness varying between 19 and 28 (Table S2). The C1a sample, which is the only quadrat located on the west side of the edifice, displayed the highest taxonomic richness with the occurrence of 32 taxa, while R2 showed only 12 taxa among 133 identified specimens (Fig. 4; Table S2). Macrofaunal communities were dominated by six taxa: the engineer species *Bathymodiolus azoricus* and its commensal worm *Branchipolynoe seepensis*, the polychaete *Amphisamytha lutzi* and three species of gastropods *Lepetodrilus atlanticus*, *Protolira valvatoides* and *Pseudorimula midatlantica*. Together, they accounted for 68.3 ± 15.7% of the total abundance. The nematode *Oncholaimus dyvae* and copepod *Aphotopontius sp*., which are typical meiofaunal species, were also abundant in the > 250 µm fraction of most samples. In the pre-disturbed community, ~74% of taxa (e.g. 29 taxa over 43) showed low occurrence and abundance (i.e. below 1% frequency) in the different samples (Table S3).

A RDA has been performed to identify the role of environmental conditions on faunal distribution and verify the temporal stability of baseline communities. The RDA model performed on Hellinger-transformed species densities accounted for 49.6% (adjusted R^2: 25.1%, p = 0.008) of the total inertia in macrofaunal species assemblage structure (Fig. 5). The overall RDA model was significant (*p-value* = 0.004) and only the first axis was significant (p = 0.05), accounting for 20% of the variation in community structure. Maximum temperature (T.max) and total dissolved sulphide concentrations (TdS) were the significant environmental factors influencing macrofaunal composition (p = 0.009 and 0.021, respectively). The years at which the samples were collected did not explain the differences between quadrats. R2cg sample stood out from the other sampling locations and was characterised by a high relative density of the gastropod *Lurifax vitreus*, contrasting with a low density of *B. azoricus* (Fig. 5). Moreover, the C2acg and R0b samples, characterised by a high density of amphipods (*Luckia striki*), formed a distinct group (Fig. 5). All other samples showed a quite homogeneous faunal composition.

3.3. Recovery patterns of benthic communities

Recolonisation dynamics of the foundation species – The recovery rate of *Bathymodiolus azoricus*, in terms of density, varied between 9.7% and 37.6% on the different quadrats one year after disturbance, and from 1.9% to 33% two years after disturbance (Fig. 6). No significant difference can be noticed between the mean recovery rate after 1 year (19.8 ± 13%) and 2 years of recolonisation (14.4 ± 13.5%) (Student test: t = 0.59, *p-value* = 0.58). However, with the exception of the C2bcg quadrat, the percentage of recovery was slightly higher in the quadrats that were caged during the recolonisation process (>20%) compared to the uncaged quadrats (<15%) (Fig. 6). The size population structure analyses of *B. azoricus* showed individuals ranging from 251 µm to 8.5 cm length within the different assemblages (Fig. 6). The pre-disturbed structure of the population on Montségur showed a polymodal size distribution dominated by a large proportion (i.e. 52% of the overall population) of small individuals below 5 mm in shell-length and a tail of distribution in larger sizes containing several cohorts (Fig. 6). Pairwise Kolmogorov-Smirnov distribution tests showed significant differences in population size structure between the pre-disturbed and post-disturbance communities in all samples (*p-value* < 0.001), except C2b (D = 0.10, *p-value* = 0.13) (Fig. 6). Furthermore, Wilcoxon-Mann-Whitney tests highlighted that the mean shell length of *B. azoricus* was smaller 1 and 2 years after the disturbance compared to that of the pre-disturbed community for all samples except C1a and C2b (Fig. 6). Furthermore, the proportion of juveniles of *B. azoricus* (< 5 mm) in the overall population was higher in assemblages sampled 1 year (67%) and two years (70%) after the disturbance in comparison to pre-disturbed populations (52%) (Table S3).

Recolonisation dynamics of active vent communities – The rarefaction curves did not level off for most of the post-disturbance samples on Montségur, but they show similar trends than that of pre-disturbed communities (Fig. S3). The shape of the curves indicate that they should reach a plateau earlier, highlighting a higher evenness in the recovering communities. Species richness (S) is lower (from 1 to 6 less species) in the post-disturbance assemblages compared to the pre-disturbed communities 1 year after the induced disturbance (Fig. 4A, Table S2). On the other hand, two years after, the C2a and C2acg quadrats showed a higher species richness than pre-disturbed quadrats, while C2b and C2bcg exhibited lower values after the disturbance (Fig. 4A, Table S2). Overall, species richness was homogeneous between all samples and was not significantly different along the recolonisation process (Kruskal-Wallis

test: P= 1.17, *p-value* = 0.56, Fig. 4A). However, macrofaunal densities were significantly lower after 1 year (15 768 ± 12 487 ind.m^{-2}) and 2 years (11 190 ± 8 270 ind.m^{-2}) after the disturbance, in comparison to the pre-disturbed community (34 402 ± 7 590 ind.m^{-2}) (Kruskal-Wallis test: P= 7.65, *p-value* = 0.021 and Post hoc Dunn test: *p-value* < 0.05, Fig. 4A) with a density recovery rate ranging from 15.7% on C1b after 1 year to 79.6% on C2acg 2 years after the disturbance (Fig. 6, Table S2). The Shannon index and Pielou's evenness were highly variable across samples in the pre-disturbed communities, but higher 1 year and 2 years after the disturbance (Fig. 4C and 4D, Table S2). Overall Pielou's evenness index is significantly higher in post-disturbance communities compared to pre-disturbed communities (Kruskal-Wallis test: P= 7.34, *p-value* = 0.026 and Post hoc Dunn test: *p-value* < 0.05, Fig. 4D). In the same way, the proportion of low occurrence species is lower in post-disturbance communities (60% after 1 year and 58% after 2 years) than prior to the induced disturbance (74%) (Table S2).

The output of the RDA computed on Hellinger-transformed densities of the different species along the recolonisation process showed a significant difference in faunal composition between the pre-disturbed communities and post-disturbance communities at Montségur (Fig. 7). The RDA model explained 42% (Adjusted R^2 = 20.5%) of the total inertia in species assemblage structure (*p-value* = 0.006). The main driver of this observed difference is time after the induced disturbance (*p-value* = 0.001), whereas no significant cage effect or dependence between sites were observed (p-values = 0.300 and 0.262, respectively). The analysis of similarity (ANOSIM) on Bray-Curtis dissimilarity matrix suggests a major change in macrofaunal composition between pre-disturbed communities and those after 1 and 2 years of recolonisation (R = 0.712, *p-value* = 0.001). However, no significant difference in faunal composition was identified between the assemblages collected 1 year and those collected 2 years after the disturbance.

Some species appeared to play a major role in the observed differences along the recolonisation process (Fig. 8). Indeed, a decrease in the abundance of the typical vent species (*Bathymodiolus azoricus*, *Branchipolynoe seepensis*, *Amphisamytha lutzi* and *Lepetodrilus atlanticus)* was observed in the post-disturbance communities, while small gastropod species (i.e. *Lurifax vitreus*, *Protolira valvatoides*, *Laeviphitus desbruyeresi*, *Xylodiscula analoga*) and nematodes (*Oncholaimus dyvae*) showed a significant increase in the post-disturbance

communities (Fig. 8, Fig. S4). *Pseudorimula midatlantica* and the copepod *Aphotopontius sp.* displayed higher relative abundances in the first year after the disturbance in comparison to the pre-disturbed community and returned to lower values 2 years after the disturbance. As observed for *B. azoricus,* the other dominant species displayed a polymodal structure of size distribution and differences have been identified between the pre-disturbed community and post disturbance state (pairwise Kolmogorov-Smirnov test) (Fig. S4). Furthermore, individuals of *A. lutzi*, *B. seepensis, L. lepetodrilus* and *P. valvatoides* were overall smaller within the communities after disturbance in comparison to those of the pre-disturbed community in most quadrats (Fig. S4). For *P. midatlantica*, only 1 quadrat showed significant differences in population size structure (Fig. S4).

4. Discussion

In this study, we provide an early evaluation of the recovery of deep-sea benthic communities to a small-scale (<1 m^2) disturbance experiment at an active hydrothermal edifice located on the Lucky Strike vent field. The structure of pre-disturbed communities and their recovery patterns were characterised through the analysis of faunal composition, diversity, population size structure in relation to biotic and abiotic factors at the Montségur edifice. This experimental design represents an innovative approach to assess the recovery of vent communities in areas where opportunities to observe natural disturbances are rare. It provides useful insights about local recolonisation drivers at hydrothermal vents, data that can contribute to the elaboration of conservation strategies in the context of potential deep-sea mining activities on seafloor massive sulphides.

4.1. Habitat characterisation

In active vent ecosystems, environmental factors are strongly linked to the output flux and chemistry of hydrothermal fluids and the resulting physico-chemical conditions along the mixing gradient between vent fluids and surrounding sea water. Within the active habitats sampled in this study, mean temperature among *Bathymodiolus azoricus* faunal assemblages varied from 5.2 to 9.5 °C with a maximum of 22.1 °C, which corresponds to the temperature ranges of Eiffel Tower habitats (Husson et al. 2017, Sarrazin et al. 2020). We identified two microhabitats hosting *B. azoricus* assemblages, which have previously been described as cold and warm habitats in Sarrazin et al. (2015). However, while in our study these habitats are

colonised by mussels, in the previous study warm habitats were rather reported to be associated with shrimp assemblages. This discrepancy could be related to temperature measurements: in the present study, temperature was measured using iButtons^{TM} deployed on or within the mussels while most measurements reported previously were conducted using the ROV probe placed a few millimeters above the faunal assemblages (Cuvelier et al. 2014a, Husson et al. 2017, Sarrazin et al. 2015, 2020). The rapid mixing of the warm fluids with the above cold seawater can account for these differences. Similar to previous studies, most samples belonging to the cold habitat showed small variability in environmental conditions and were associated with low temperature, low concentrations of iron and sulphides, high pH and high concentrations of dissolved oxygen (Cuvelier et al. 2011a; Sarrazin et al. 2015). However, a few quadrats (R1, C2a and R0b) were characterised by higher temperatures, total dissolved sulphide and iron concentrations as well as lower dissolved oxygen concentrations with acidic pH, which are more representative of warm habitats.

The continuous bi-hourly monitoring of temperature revealed a high spatial variability in temperature regime (up to 3°C across 10 cm), suggesting the occurrence of multiple microhabitats within a single quadrat. This was supported by high standard deviation values of replicate measurements for sulphides and iron concentrations performed every year. This small-scale temporal variability of temperature can be a result of several processes, including the interplay between sulphide and oxygen biological uptake (Johnson et al., 1988), the formation of diffuse fluids in the subsurface, the chemical reactivity of the mixing zone, the porosity of the substratum in active habitats on the East Pacific Rise (Butterfield et al. 1990; Sarrazin et al. 2002, Le Bris et al. 2006) or tidal oscillations (Barreyre et al. 2014). Our results show significant semi-diurnal and diurnal periods and harmonics, supporting the presence of periodic oscillations related to tidal processes. Tidal modulation of diffused-flow has been reported in many vent systems (Cuvelier et al., 2014b; Sarrazin et al., 2014; Scheirer et al., 2006). These variations are mainly caused by tidally induced currents (Barreyre et al., 2014; Khripounoff et al., 2008) and changes in hydrostatic pressure on the seafloor (Davis and Becker, 1999). This periodicity could be beneficial for symbiotic sessile species that need alternative inputs of reduced compounds and oxygen to ensure chemosynthesis (Scheirer et al. 2006, Mat et al. 2020) but can also influence the behaviour of mobile species (Lelièvre et al., 2017).

4.2. Pre-disturbed communities and natural variability

On the active Montségur edifice, all experimental quadrats were visually dominated by medium-sized *B. azoricus* mussels from 5.2 ± 8.8 mm to 24.4 ± 14.3 mm. These sizes are consistent with the mean lengths reported by Comtet and Desbruyères (1998) on different edifices of Lucky Strike (between 5.63 ± 5.67 mm and 49.63 ± 31.41 mm), but smaller than those measured by Sarrazin et al. (2015) on the nearby Eiffel Tower edifice (between 22.7 ± 18.07 and 74.7 ± 2.57 mm). Indeed, we observed a high proportion (between 52 and 96%) of very small individuals -below 3 mm- in each sample, sizes that correspond to post larval and juvenile stages. The presence of several successive cohorts suggests the occurrence of a massive recruitment event around June, just before sampling. These results are consistent with the lifecycle of *B. azoricus*, with an annual spawning event in January followed by a planktotrophic larval development and the settlement of post-larvae in May-June (Colaço et al., 2006; Comtet and Desbruyères, 1998; Dixon et al., 2006). Furthermore, differences in mean shell length of *B. azoricus* observed among samples on pre-disturbed communities may be due to spatial segregation of sizes related to environmental factors (Sarrazin et al., 2015; Husson et al., 2017) or to biotic interactions (e.g. competition, predation) that may play an important role in recruitment success and survival of post-larvae (Lenihan et al., 2008; Sancho et al., 2005).

All samples collected at the active Montségur edifice were dominated by the same macrofaunal species (e.g. *B. azoricus*, *B. seepensis*, *A. lutzi*, *P. valvatoides* and *L. atlanticus*), which have been previously described as indicator species of cold microhabitats on the Eiffel Tower edifice situated ~ 50 m from Montségur (Sarrazin et al., 2015b). The high similarity between the fauna from the two edifices may be related to their belonging to the same chemistry domain (Chavagnac et al. 2018, Sarrazin et al. 2020). Among the 43 macrofaunal species identified on Montségur, approximately 74% exhibit a low frequency of abundance (<1%). Total densities of organisms in the pre-disturbed communities ranged from 3 330 to 68 960 ind.m^{-2} across the different samples, and is much lower than the values reported by Sarrazin et al. (2020) on the same edifice (between 62 253 and 126 437 ind.m-2). In several studies, small mussel assemblages, inhabiting cold microhabitats, harbour higher density and

diversity of associated species than large mussel assemblages, found in warmer microhabitats (Cuvelier et al., 2009; Dreyer et al., 2005; Sarrazin et al., 2015). Surprisingly, in this study the highest densities of organisms have been observed in the warmest and more variable habitats. This result may be linked to the differences in the method for assessing temperature as mentioned above. Indeed, temperature values obtained by probes deployed directly on the substratum are expected to be higher than the ones obtained with the ROV probe a few millimeters above faunal assemblages.

As expected, macrofaunal distribution was significantly influenced by environmental conditions, especially by mean temperature and mean concentrations in total sulphides and methane, in addition to slightly acidic conditions (pH <7.3). However, biotic factors such as competition for space and food resource, but also predation or facilitation, may also play an important role in faunal distribution in diffuse flow habitats (Sarrazin et al. 1997, Sen et al. 2013; Gollner et al. 2015b; Husson et al. 2017). On the other hand, faunal composition within reference quadrats did not differ over the three years of the experiment, suggesting a relative stability of the community over time. This supports the observed high stability of mussel communities on the nearby Eiffel Tower edifice, which led to the assumption that *B. azoricus* assemblages at Lucky Strike can be considered as a "climax" community (Cuvelier et al., 2011b). The absence of natural changes in faunal assemblages, at the edifice scale, during the experiment allows us to use them as a baseline to test the effect of the induced disturbance on benthic communities.

4.3. Recolonisation processes and recovery

In Figure 9, we propose a succession model of nMAR vent communities based on the present experiment at the Lucky Strike vent field and from previous studies conducted after natural disturbances at vents. The first step after the disturbance relies on the release of an ecological niche induced by the removing of faunal assemblages. Then, the stabilisation of environmental conditions, especially of temperature and reduced compounds, would allow chemoautotrophic primary production and proliferation of microbial mats, as observed in studies from vents in the Pacific Ocean (Marcus et al., 2009; Shank et al., 1998; Tunnicliffe et al., 1997). This is followed, within one year, by the arrival of mobile opportunistic species,

including shrimps and copepod species. Although not significant, our results suggest that these predator species may slow down the settlement of associated species, resulting in a poor recovery of faunal densities despite a good species richness recovery. Two years after the disturbance, the settlement of several gastropod species grazing on free-living microbial mats have been observed. At this stage, the higher Pielou's evenness compared to baseline communities suggests that biotic interactions are not yet fully effective within assemblages. Gastropods have already been described as main pioneer colonists at 9°N EPR after the 2006 volcanic eruption (Mullineaux et al., 2012, 2010). Indeed, despite contrasting reproductive characteristics, some of them are able to maintain an important effective population size and support high abundances, especially through an early maturity and continuous gametogenesis (Marticorena et al., 2020). Thereafter, we hypothesise a later settlement of the foundation species *B. azoricus* due to its seasonal reproduction, which leads to a single recruitment event in June (Colaço et al., 2006; Dixon et al., 2006). The recolonisation of *B. azoricus* can occur through recruitment events and settlement of post-larvae and juveniles or by immigration of mobile adults from nearby assemblages (Comtet and Desbruyères, 1998). Indeed, observations made on imagery on the Eiffel Tower edifice showed that *B. azoricus* is able to move several centimetres a day (Matabos, Sarrazin, unpublished data). Since the growth rate of B. azoricus juveniles has been estimated to reach ~ 2 mm per year on the Eiffel Tower edifice (from imagery analysis, Sarrazin and Matabos unpublished data), we can assume that the presence of mussels larger than 1 cm after 1 and 2 years of recolonisation is most probably a result of adult migration. On the other hand, the mean shell length of *B. azoricus* was significantly lower and a higher proportion of juveniles were observed on post-disturbance assemblages compared to pre-disturbed communities. This suggests that within our study, the recruitment and settlement of young mussels were the main drivers of recolonisation after the disturbance, rather than migration. Moreover, the results of the predator exclusion experiment suggest that the recruitment success of *B. azoricus* might depend on predation pressure on post-larval individuals by large mobile predators (e.g. shrimp, crabs, fishes). The impact of predation on the entire benthic community could be even more significant when predators specifically feed on taxa that play a key role in the community and interact widely with other species (Paine, 1966). We also observed that the cages led to the formation of thick microbial mats on their surfaces, implying that the presence of the plastic mesh and its size may have modified the input of hydrothermal fluids. The deployment of additional "true" cage

control quadrats would be necessary to dissociate the role of predator exclusion and potentially other effects of the mesh such as hydrodynamic modifications. The establishment and growth of *B. azoricus* may then promote the settlement of low occurrence species and a rapid recovery of faunal densities through the creation of a three dimensional habitat that contributes to reduce fluid flux, making the habitat more suitable for other species (Johnson et al. 1988; Sarrazin et al. 1997, Shank et al. 1998). Finally, biotic interactions including predation, competition for space and nutritional resources and facilitation may lead to changes in faunal relative abundance and dominance before reaching an equilibrium. All these mechanisms contribute to reducing the evenness among assemblages and enhance the dominance of a few taxa (Fig. 9). Once this equilibrium is achieved, we can consider that these assemblages reach their climax. The climax community of Montségur appears to be similar to that of the neighbouring Eiffel Tower edifice (Cuvelier et al., 2011a) and some other active edifices of the Lucky Strike vent field (Sarrazin et al. 2020). These communities are characterised by the dominance of a few vent taxa and a high proportion of low occurrence species. Natural or anthropogenic disturbance events, which can occur at each step of this successional model, may lead to significant changes in faunal assemblages and even provoke community collapse, depending on their spatial breadth as proposed in different vent successional models (Sarrazin et al. 1997, Shank et al. 1998).

Several factors can come into play in recolonisation and ecological succession following a disturbance, and their relative importance changes according to the scale of disturbance (Zajac et al. 1998, Benedetti 2000). After a small-scale disturbance, recovery of vent assemblages are strongly affected by the spatio-temporal variability of environmental conditions, which may lead to local extinction or creation of new suitable habitats (Sarrazin et al. 1997; Shank et al. 1998, Marcus et al. 2009; Sen et al. 2014). Feeding strategies (Lelièvre et al. 2018; Van Audenhaege et al., 2019) and biotic interactions (i.e. competition for space, facilitation or predation) have also been identified as important drivers of faunal succession at the edifice scale (Sarrazin et al. 1997, Micheli et al. 2002; Hunt et al. 2004; Govenar and Fisher 2007; Cuvelier et al. 2014a). In this study, we showed that, at this small-scale, biological interactions are more likely to play a predominant role in faunal succession rather than environmental conditions. The same observations have been noticed on vents at back-arc basins and may be due to the high stability of environmental conditions, typical of slow-spreading centers (Sen et al., 2014). Furthermore, in mosaic habitats, the diversity and species

574 composition at the boundary of disturbed patches might modulate biotic interactions and
575 migrations of individuals, influencing early stages of recovery (Bulleri et al. 2006). However,
576 diversity descriptors and faunal composition were relatively homogeneous between the
577 different quadrats at each step of the recolonisation process, suggesting that succession after
578 small-scale disturbance at Lucky Strike can be described as a deterministic sequence of species
579 replacement. As observed on rocky-shore habitats, the timing of disturbance might also affect
580 recolonisation patterns (Sousa 1985, Benedetti and Cinelli 1996). For example, *B. azoricus*
581 have been described to recruit seasonally around the month of June (Dixon et al. 2006; Colaço
582 et al. 2006) and the occurrence of disturbance in spring might result in a faster recovery of
583 assemblages and less importance of gastropods in the first stage of recolonisation.
584

585 ## 5. Conclusion

586 We designed a novel *in situ* experimental approach to identify biotic and abiotic factors driving
587 the recolonisation and succession of vent communities after a small-scale disturbance.
588 Recolonisation dynamics was strongly affected by species composition of the neighbouring
589 faunal assemblages. Biotic interactions were predominant and highly influenced the slow
590 recovery of vent assemblages, while environmental factors remained stable. Our results,
591 coupled with observations from literature data, lead to a first conceptual model of
592 colonisation and ecological succession for northern Mid-Atlantic communities.
593

594 At regional scales (i.e. vent field), life-history traits including reproduction (Kelly and Metaxas,
595 2007), larval dispersal modes and recruitment abilities (Levin et al., 1996; Levin, 2006;
596 Mullineaux et al., 2003, 2012) constitute additional key factors that influence faunal
597 colonisation processes and subsequent successional patterns (Zajac et al., 1998; Adams et al.,
598 2012; Nakamura et al., 2014). While the recolonisation of areas following large-scale
599 disturbance relies on dispersal across vent fields, at local scale the successful settlement of
600 post-larvae depends on habitat suitability, environmental conditions and biotic interactions.
601 Understanding the processes acting at small scales are paramount in evaluating mechanisms
602 controlling successional dynamics after recolonisation by species from afar. In addition, recent
603 workshops and working groups, emerging from the development of mining regulations and
604 the necessity to inform industries and policy makers, stressed the urgent need to address

knowledge gaps in vent species biology and ecology (Collins et al. 2013; Levin et al. 2016; Dunn et al. 2018, ISA REMPS, SEMPIA). This study is one of the first to assess natural recovery of communities on a slow-spreading ridge and provide data that are essential to elaborate and develop conservation strategies and mitigate long-term harmful effects of anthropogenic activities on hydrothermal vent ecosystems.

DOI of cruises involved

SARRADIN Pierre-Marie, CANNAT Mathilde (2017) MOMARSAT2017 cruise, RV Pourquoi pas ?, https://doi.org/10.17600/17000500

CANNAT Mathilde (2018) MOMARSAT2018 cruise, RV L'Atalante, https://doi.org/10.17600/18000514

SARRADIN Pierre-Marie, LEGRAND Julien (2019) MOMARSAT2019 cruise, RV Pourquoi pas ?, https://doi.org/10.17600/18001110

Acknowledgements

We would like to thank the captains and crews of the oceanographic cruises Momarsat 2017, 2018 and 2019 aboard the vessels N/O Pourquoi pas? and L'Atalante, as well as the ROV Victor6000 and Nautile team. We are particularly grateful to Pierre-Marie Sarradin and Mathilde Cannat, chief scientists of the cruises who greatly supported our sampling program. We are also sincerely thankful to Philippe Rodier for instrumental design of pyramidal structure and cage experiment but also for the deployment of the reversing thermometer and the data acquisition of bottom sea water temperature. We would like to offer our special thanks to Sandra Fuchs and Fanny Girard for sample collection during the cruise and Julie Tourolle for providing the map captions. We are particularly grateful for the assistance given by Thomas Day, Mathilde Le Pans, Maureen Lapalme and Fanny Volage in sorting and morphometrical measurements. Finally, we wish to acknowledge the help provided for specimen identification by the taxonomists Dr Paulo Bonifácio and Dr Maurício Shimabukuro for polychaetes, Dr Anders Warén for gastropods, Dr Inmaculada Frutos for isopods, Dr Magdalena Błażewicz for tanaids, Dr Laure Corbari for amphipods and Dr Hayato Tanaka for ostracods. This research was supported by the European H2020 MERCES (Project ID 689518) and the eCOREF project funded by Equinor (Norway). Julien Marticorena PhD project was funded by Ifremer and Equinor. This project is part of the EMSO-Azores (https://www.emso-fr.org) regional node and EMSO ERIC Research Infrastructure (https://emso.eu/). ERLL was supported by the European H2020 MERCES (Project ID 689518).

References

Adams, D.K., Arellano, S.M., Govenar, B., 2012. Larval dispersal : vent life in the water column. https://doi.org/10.5670/oceanog.2012.24

Anderson, M.J., 2001. A new method for non-parametric multivariate analysis of variance. Austral Ecol. 26, 32–46. https://doi.org/10.1111/j.1442-9993.2001.01070.pp.x

643 Baco, A.R., Etter, R.J., Ribeiro, P.A., Heyden, S. von der, Beerli, P., Kinlan, B.P., 2016. A synthesis of
644 genetic connectivity in deep-sea fauna and implications for marine reserve design. Mol. Ecol. 25, 3276–
645 3298. https://doi.org/10.1111/mec.13689

646 Barreyre, T., Escartín, J., Sohn, R.A., Cannat, M., Ballu, V., Crawford, W.C., 2014. Temporal variability
647 and tidal modulation of hydrothermal exit-fluid temperatures at the Lucky Strike deep-sea vent field,
648 Mid-Atlantic Ridge. J. Geophys. Res. Solid Earth 119, 2543–2566.
649 https://doi.org/10.1002/2013JB010478

650 Beaulieu, S.E., Baker, E.T., German, C.R., 2015. Where are the undiscovered hydrothermal vents on
651 oceanic spreading ridges? Deep Sea Res. Part II Top. Stud. Oceanogr., Exploring New Frontiers in Deep-
652 Sea Research: In Honor and Memory of Peter A. Rona 121, 202–212.
653 https://doi.org/10.1016/j.dsr2.2015.05.001

654 Benedetti-Cecchi, L., Cinelli, F., 1996. Patterns of disturbance and recovery in littoral rock pools:
655 nonhierarchical competition and spatial variability in secondary succession. Marine Ecology Progress
656 Series 135, 145–161. https://doi.org/10.3354/meps135145

657 Benedetti-Cecchi, L., 2000. Predicting Direct and Indirect Interactions During Succession in a Mid-
658 Littoral Rocky Shore Assemblage. Ecological Monographs 70, 45–72. https://doi.org/10.1890/0012-
659 9615(2000)070[0045:PDAIID]2.0.CO;2

660 Boschen, R.E., Rowden, A.A., Clark, M.R., Gardner, J.P.A., 2013. Mining of deep-sea seafloor massive
661 sulfides: A review of the deposits, their benthic communities, impacts from mining, regulatory
662 frameworks and management strategies. Ocean Coast. Manag. 84, 54–67.
663 https://doi.org/10.1016/j.ocecoaman.2013.07.005

664 Breusing, C., Biastoch, A., Drews, A., Metaxas, A., Jollivet, D., Vrijenhoek, R.C., Bayer, T., Melzner, F.,
665 Sayavedra, L., Petersen, J.M., Dubilier, N., Schilhabel, M.B., Rosenstiel, P., Reusch, T.B.H., 2016.
666 Biophysical and Population Genetic Models Predict the Presence of “Phantom” Stepping Stones
667 Connecting Mid-Atlantic Ridge Vent Ecosystems. Curr. Biol. CB 26, 2257–2267.
668 https://doi.org/10.1016/j.cub.2016.06.062

669 Bulleri, F., Benedetti-Cecchi, L., 2006. Mechanisms of recovery and resilience of different components
670 of mosaics of habitats on shallow rocky reefs. Oecologia 149. https://doi.org/10.1007/s00442-006-
671 0459-3

672 Butterfield, D.A., Jonasson, I.R., Massoth, G.J., Feely, R.A., Roe, K.K., Embley, R.E., Holden, J.F., McDuff,
673 R.E., Lilley, M.D., Delaney, J.R., 1997. Seafloor eruptions and evolution of hydrothermal fluid chemistry.
674 Philos. Trans. R. Soc. Lond. Ser. Math. Phys. Eng. Sci. 355, 369–386.
675 https://doi.org/10.1098/rsta.1997.0013

676 Butterfield, D.A., Massoth, G.J., McDuff, R.E., Lupton, J.E., Lilley, M.D., 1990. Geochemistry of
677 hydrothermal fluids from Axial Seamount hydrothermal emissions study vent field, Juan de Fuca Ridge:
678 Subseafloor boiling and subsequent fluid-rock interaction. J. Geophys. Res. Solid Earth 95, 12895–
679 12921. https://doi.org/10.1029/JB095iB08p12895

680 Chavagnac, V., Leleu, T., Fontaine, F., Cannat, M., Ceuleneer, G., Castillo, A., 2018. Spatial Variations in
681 Vent Chemistry at the Lucky Strike Hydrothermal Field, Mid-Atlantic Ridge (37°N): Updates for
682 Subseafloor Flow Geometry From the Newly Discovered Capelinhos Vent. Geochemistry, Geophysics,
683 Geosystems 19, 4444–4458. https://doi.org/10.1029/2018GC007765

Childress, J.J., Fisher, C.R., 1992. The biology of hydrothermal vent animals: physiology, biochemistry, and autotrophic symbioses. Unkn. J. 337–441.

Colaço, A., Martins, I., Laranjo, M., Pires, L., Leal, C., Prieto, C., Costa, V., Lopes, H., Rosa, D., Dando, P.R., Serrão-Santos, R., 2006. Annual spawning of the hydrothermal vent mussel, Bathymodiolus azoricus, under controlled aquarium, conditions at atmospheric pressure. J. Exp. Mar. Biol. Ecol. 333, 166–171. https://doi.org/10.1016/j.jembe.2005.12.005

Collins, P.C., Kennedy, R., Van Dover, C.L., 2012. A biological survey method applied to seafloor massive sulphides (sms) with contagiously distributed hydrothermal-vent fauna. https://doi.org/10.3354/meps09646

Comtet, T., Desbruyères, D., 1998. Population structure and recruitment in mytilid bivalves from the Lucky Strike and Menez Gwen hydrothermal vent fields (37°17\'N and 37°50\'N on the Mid-Atlantic Ridge). Mar. Ecol. Prog. Ser. 163, 165–177. https://doi.org/10.3354/meps163165

Connell, J.H., Keough, M.J., 1985. Disturbance and patch dynamics of subtidal marine animals on hard substrata.

Corliss, J.B., Dymond, J., Gordon, L.I., Edmond, J.M., Herzen, R.P. von, Ballard, R.D., Green, K., Williams, D., Bainbridge, A., Crane, K., Andel, T.H. van, 1979. Submarine Thermal Springs on the Galápagos Rift. Science 203, 1073–1083. https://doi.org/10.1126/science.203.4385.1073

Cuvelier, D., Beesau, J., Ivanenko, V.N., Zeppilli, D., Sarradin, P.-M., Sarrazin, J., 2014a. First insights into macro- and meiofaunal colonisation patterns on paired wood/slate substrata at Atlantic deep-sea hydrothermal vents. Deep Sea Res. Part Oceanogr. Res. Pap. 87, 70–81. https://doi.org/10.1016/j.dsr.2014.02.008

Cuvelier, D., Gollner, S., Jones, D.O.B., Kaiser, S., Arbizu, P.M., Menzel, L., Mestre, N.C., Morato, T., Pham, C., Pradillon, F., Purser, A., Raschka, U., Sarrazin, J., Simon-Lledó, E., Stewart, I.M., Stuckas, H., Sweetman, A.K., Colaço, A., 2018. Potential Mitigation and Restoration Actions in Ecosystems Impacted by Seabed Mining. Front. Mar. Sci. 5. https://doi.org/10.3389/fmars.2018.00467

Cuvelier, D., Legendre, P., Laes, A., Sarradin, P.-M., Sarrazin, J., 2014b. Rhythms and Community Dynamics of a Hydrothermal Tubeworm Assemblage at Main Endeavour Field – A Multidisciplinary Deep-Sea Observatory Approach. PLOS ONE 9, e96924. https://doi.org/10.1371/journal.pone.0096924

Cuvelier, D., Sarradin, P.-M., Sarrazin, J., Colaço, A., Copley, J.T., Desbruyères, D., Glover, A.G., Santos, R.S., Tyler, P.A., 2011a. Hydrothermal faunal assemblages and habitat characterisation at the Eiffel Tower edifice (Lucky Strike, Mid-Atlantic Ridge). Mar. Ecol. 32, 243–255. https://doi.org/10.1111/j.1439-0485.2010.00431.x

Cuvelier, D., Sarrazin, J., Colaço, A., Copley, J., Desbruyères, D., Glover, A.G., Tyler, P., Serrão Santos, R., 2009. Distribution and spatial variation of hydrothermal faunal assemblages at Lucky Strike (Mid-Atlantic Ridge) revealed by high-resolution video image analysis. Deep Sea Res. Part Oceanogr. Res. Pap. 56, 2026–2040. https://doi.org/10.1016/j.dsr.2009.06.006

Cuvelier, D., Sarrazin, J., Colaço, A., Copley, J.T., Glover, A.G., Tyler, P.A., Santos, R.S., Desbruyères, D., 2011b. Community dynamics over 14 years at the Eiffel Tower hydrothermal edifice on the Mid-Atlantic Ridge. Limnol. Oceanogr. 56, 1624–1640. https://doi.org/10.4319/lo.2011.56.5.1624

Davis, E., Becker, K., 1999. Tidal pumping of fluids within and from the oceanic crust: New observations and opportunities for sampling the crustal hydrosphere. Earth Planet. Sci. Lett. 172, 141–149. https://doi.org/10.1016/S0012-821X(99)00197-1

Denny, M.W., 1987. Lift as a mechanism of patch initiation in mussel beds. Journal of Experimental Marine Biology and Ecology 113, 231–245. https://doi.org/10.1016/0022-0981(87)90103-1

Dixon, D.R., Lowe, D.M., Miller, P.I., Villemin, G.R., Colaço, A., Serrão-Santos, R., Dixon, L.R.J., 2006. Evidence of seasonal reproduction in the Atlantic vent mussel Bathymodiolus azoricus, and an apparent link with the timing of photosynthetic primary production. J. Mar. Biol. Assoc. U. K. 86, 1363–1371. https://doi.org/10.1017/S0025315406014391

Donval, J.-P., Charlou, J.-L., Lucas, L., 2008. Analysis of light hydrocarbons in marine sediments by headspace technique: Optimization using design of experiments. Chemometrics and Intelligent Laboratory Systems 94, 89–94. https://doi.org/10.1016/j.chemolab.2008.06.010

Dray, S., Bauman, D., Blanchet, G., Borcard, D., Clappe, S., Guenard, G., Jombart, T., Larocque, G., Legendre, P., Madi, N., Wagner, H.H., 2020. adespatial: Multivariate Multiscale Spatial Analysis.

Dreyer, J.C., Knick, K.E., Flickinger, W.B., Dover, C.L.V., 2005. Development of macrofaunal community structure in mussel beds on the northern East Pacific Rise. Mar. Ecol. Prog. Ser. 302, 121–134. https://doi.org/10.3354/meps302121

Dunn, D.C., Dover, C.L.V., Etter, R.J., Smith, C.R., Levin, L.A., Morato, T., Colaço, A., Dale, A.C., Gebruk, A.V., Gjerde, K.M., Halpin, P.N., Howell, K.L., Johnson, D., Perez, J.A.A., Ribeiro, M.C., Stuckas, H., Weaver, P., Participants, S.W., 2018. A strategy for the conservation of biodiversity on mid-ocean ridges from deep-sea mining. Science Advances 4, eaar4313. https://doi.org/10.1126/sciadv.aar4313

Kassambara and Mundt, 2009. Factoextra: Extract and Visualize the Results of Multivariate Data Analyses, 2019. , R package.

Gollner, S., Govenar, B., Arbizu, P.M., Mills, S., Le Bris, N., Weinbauer, M., Shank, T.M., Bright, M., 2015a. Differences in recovery between deep-sea hydrothermal vent and vent-proximate communities after a volcanic eruption. Deep Sea Res. Part Oceanogr. Res. Pap. 106, 167–182. https://doi.org/10.1016/j.dsr.2015.10.008

Gollner, S., Riemer, B., Arbizu, P.M., Bris, N.L., Bright, M., 2010. Diversity of Meiofauna from the 9°50'N East Pacific Rise across a Gradient of Hydrothermal Fluid Emissions. PLOS ONE 5, e12321. https://doi.org/10.1371/journal.pone.0012321

Gollner, S., Govenar, B., Fisher, C.R., Bright, M., 2015b. Size matters at deep-sea hydrothermal vents: different diversity and habitat fidelity patterns of meio- and macrofauna. Mar. Ecol. Prog. Ser. 520, 57–66. https://doi.org/10.3354/meps11078

Gollner, S., Kaiser, S., Menzel, L., Jones, D.O.B., Brown, A., Mestre, N.C., van Oevelen, D., Menot, L., Colaço, A., Canals, M., Cuvelier, D., Durden, J.M., Gebruk, A., Egho, G.A., Haeckel, M., Marcon, Y., Mevenkamp, L., Morato, T., Pham, C.K., Purser, A., Sanchez-Vidal, A., Vanreusel, A., Vink, A., Martinez Arbizu, P., 2017. Resilience of benthic deep-sea fauna to mining activities. Mar. Environ. Res. 129, 76–101. https://doi.org/10.1016/j.marenvres.2017.04.010

Gollner, S., Govenar, B., Martinez Arbizu, P., Mullineaux, L.S., Mills, S., Le Bris, N., Weinbauer, M., Shank, T.M., Bright, M., 2020. Animal Community Dynamics at Senescent and Active Vents at the 9°N

East Pacific Rise After a Volcanic Eruption. Front. Mar. Sci. 6. https://doi.org/10.3389/fmars.2019.00832

Govenar, B., Fisher, C.R., 2007. Experimental evidence of habitat provision by aggregations of Riftia pachyptila at hydrothermal vents on the East Pacific Rise. Mar. Ecol. 28, 3–14. https://doi.org/10.1111/j.1439-0485.2007.00148.x

Hunt, H.L., Metaxas, A., Jennings, R.M., Halanych, K.M., Mullineaux, L.S., 2004. Testing biological control of colonization by vestimentiferan tubeworms at deep-sea hydrothermal vents (East Pacific Rise, 9°50'N). Deep Sea Res. Part Oceanogr. Res. Pap. 51, 225–234. https://doi.org/10.1016/j.dsr.2003.10.008

Husson, B., Sarradin, P.-M., Zeppilli, D., Sarrazin, J., 2017. Picturing thermal niches and biomass of hydrothermal vent species. Deep Sea Res. Part II Top. Stud. Oceanogr., Advances in deep-sea biology: biodiversity, ecosystem functioning and conservation 137, 6–25. https://doi.org/10.1016/j.dsr2.2016.05.028

Johnson, K.S., Childress, J.J., Beehler, C.L., 1988. Short-term temperature variability in the Rose Garden hydrothermal vent field: an unstable deep-sea environment. Deep Sea Res. Part Oceanogr. Res. Pap. 35, 1711–1721. https://doi.org/10.1016/0198-0149(88)90045-3

Jollivet, D., Empis, A., Baker, M.C., Hourdez, S., Comtet, T., Jouin-Toulmond, C., Desbruyères, D., Tyler, P.A., 2000. Reproductive biology, sexual dimorphism, and population structure of the deep sea hydrothermal vent scale-worm, Branchipolynoe seepensis (Polychaeta: Polynoidae). Journal of the Marine Biological Association of the United Kingdom 80, 55–68. https://doi.org/10.1017/S0025315499001563

Kelly, N.E., Metaxas, A., 2007. Influence of habitat on the reproductive biology of the deep-sea hydrothermal vent limpet Lepetodrilus fucensis (Vetigastropoda: Mollusca) from the Northeast Pacific. Mar. Biol. 151, 649–662. https://doi.org/10.1007/s00227-006-0505-z

Khripounoff, A., Vangriesheim, A., Crassous, P., Segonzac, M., Lafon, V., Warén, A., 2008. Temporal variation of currents, particulate flux and organism supply at two deep-sea hydrothermal fields of the Azores Triple Junction. Deep Sea Res. Part Oceanogr. Res. Pap. 55, 532–551. https://doi.org/10.1016/j.dsr.2008.01.001

Langmuir, C., Humphris, S., Fornari, D., Van Dover, C., Von Damm, K., Tivey, M.K., Colodner, D., Charlou, J.-L., Desonie, D., Wilson, C., Fouquet, Y., Klinkhammer, G., Bougault, H., 1997. Hydrothermal vents near a mantle hot spot: the Lucky Strike vent field at 37°N on the Mid-Atlantic Ridge. Earth Planet. Sci. Lett. 148, 69–91. https://doi.org/10.1016/S0012-821X(97)00027-7

Le Bris, N., Govenar, B., Le Gall, C., Fisher, C.R., 2006. Variability of physico-chemical conditions in 9°50'N EPR diffuse flow vent habitats. Mar. Chem. 98, 167–182. https://doi.org/10.1016/j.marchem.2005.08.008

Leibold, M.A., Holyoak, M., Mouquet, N., Amarasekare, P., Chase, J.M., Hoopes, M.F., Holt, R.D., Shurin, J.B., Law, R., Tilman, D., Loreau, M., Gonzalez, A., 2004. The metacommunity concept: a framework for multi-scale community ecology. Ecology Letters 7, 601–613. https://doi.org/10.1111/j.1461-0248.2004.00608.x

Lelièvre, Y., Legendre, P., Matabos, M., Mihály, S., Lee, R.W., Sarradin, P.-M., Arango, C.P., Sarrazin, J., 2017. Astronomical and atmospheric impacts on deep-sea hydrothermal vent invertebrates. Proc. R. Soc. B Biol. Sci. 284, 319–407. https://doi.org/10.1098/rspb.2016.2123

Lenihan, H.S., Mills, S.W., Mullineaux, L.S., Peterson, C.H., Fisher, C.R., Micheli, F., 2008. Biotic interactions at hydrothermal vents: Recruitment inhibition by the mussel Bathymodiolus thermophilus. Deep Sea Res. Part Oceanogr. Res. Pap. 55, 1707–1717. https://doi.org/10.1016/j.dsr.2008.07.007

Levin, L.A., 2006. Recent progress in understanding larval dispersal: new directions and digressions. Integr. Comp. Biol. 46, 282–297. https://doi.org/10.1093/icb/icj024

Levin, L.A., Baco, A.R., Bowden, D.A., Colaco, A., Cordes, E.E., Cunha, M.R., Demopoulos, A.W.J., Gobin, J., Grupe, B.M., Le, J., Metaxas, A., Netburn, A.N., Rouse, G.W., Thurber, A.R., Tunnicliffe, V., Van Dover, C.L., Vanreusel, A., Watling, L., 2016a. Hydrothermal Vents and Methane Seeps: Rethinking the Sphere of Influence. Front. Mar. Sci. 3. https://doi.org/10.3389/fmars.2016.00072

Levin, L.A., D, T., G, T., 1996. Succession of macrobenthos in a created salt marsh. Mar. Ecol. Prog. Ser. 141, 67–82. https://doi.org/10.3354/meps141067

Levin, L.A., Mengerink, K., Gjerde, K.M., Rowden, A.A., Van Dover, C.L., Clark, M.R., Ramirez-Llodra, E., Currie, B., Smith, C.R., Sato, K.N., Gallo, N., Sweetman, A.K., Lily, H., Armstrong, C.W., Brider, J., 2016b. Defining “serious harm” to the marine environment in the context of deep-seabed mining. Mar. Policy 74, 245–259. https://doi.org/10.1016/j.marpol.2016.09.032

Luther, G.W., Rozan, T.F., Taillefert, M., Nuzzio, D.B., Di Meo, C., Shank, T.M., Lutz, R.A., Cary, S.C., 2001. Chemical speciation drives hydrothermal vent ecology. Nature 410, 813–816. https://doi.org/10.1038/35071069

Marcus, J., Tunnicliffe, V., Butterfield, D.A., 2009. Post-eruption succession of macrofaunal communities at diffuse flow hydrothermal vents on Axial Volcano, Juan de Fuca Ridge, Northeast Pacific. Deep Sea Res. Part II Top. Stud. Oceanogr., Marine Benthic Ecology and Biodiversity: A Compilation of Recent Advances in Honor of J. Frederick Grassle 56, 1586–1598. https://doi.org/10.1016/j.dsr2.2009.05.004

Marsh, L., Copley, J.T., Huvenne, V.A.I., Linse, K., Reid, W.D.K., Rogers, A.D., Sweeting, C.J., Tyler, P.A., 2012. Microdistribution of Faunal Assemblages at Deep-Sea Hydrothermal Vents in the Southern Ocean. PLoS One 7. https://doi.org/10.1371/journal.pone.0048348

Marticorena, J., Matabos, M., Sarrazin, J., Ramirez-Llodra, E., 2020. Contrasting reproductive biology of two hydrothermal gastropods from the Mid-Atlantic Ridge: implications for resilience of vent communities. Mar. Biol. 167, 109. https://doi.org/10.1007/s00227-020-03721-x

Mat, A.M., Sarrazin, J., Markov, G.V., Apremont, V., Dubreuil, C., Eché, C., Fabioux, C., Klopp, C., Sarradin, P.-M., Tanguy, A., Huvet, A., Matabos, M., 2020. Biological rhythms in the deep-sea hydrothermal mussel Bathymodiolus azoricus. Nature Communications 11, 3454. https://doi.org/10.1038/s41467-020-17284-4

Micheli, F., Peterson, C.H., Mullineaux, L.S., Fisher, C.R., Mills, S.W., Sancho, G., Johnson, G.A., Lenihan, H.S., 2002. Predation Structures Communities at Deep-Sea Hydrothermal Vents. Ecol. Monogr. 72, 365–382. https://doi.org/10.1890/0012-9615(2002)072[0365:PSCADS]2.0.CO;2

Mullineaux, L.S., Adams, D.K., Mills, S.W., Beaulieu, S.E., 2010. Larvae from afar colonize deep-sea hydrothermal vents after a catastrophic eruption. Proc. Natl. Acad. Sci. 107, 7829–7834. https://doi.org/10.1073/pnas.0913187107

Mullineaux, L.S., Metaxas, A., Beaulieu, S.E., Bright, M., Gollner, S., Grupe, B.M., Herrera, S., Kellner, J.B., Levin, L.A., Mitarai, S., Neubert, M.G., Thurnherr, A.M., Tunnicliffe, V., Watanabe, H.K., Won, Y.-J., 2018. Exploring the Ecology of Deep-Sea Hydrothermal Vents in a Metacommunity Framework. Front. Mar. Sci. 5. https://doi.org/10.3389/fmars.2018.00049

Mullineaux, L.S., Bris, N.L., Mills, S.W., Henri, P., Bayer, S.R., Secrist, R.G., Siu, N., 2012. Detecting the Influence of Initial Pioneers on Succession at Deep-Sea Vents. PLOS ONE 7, e50015. https://doi.org/10.1371/journal.pone.0050015

Mullineaux, L.S., Peterson, C.H., Micheli, F., Mills, S.W., 2003. Successional Mechanism Varies Along a Gradient in Hydrothermal Fluid Flux at Deep-Sea Vents. Ecol. Monogr. 73, 523–542. https://doi.org/10.1890/02-0674

Nakamura, M., Watanabe, H., Sasaki, T., Ishibashi, J., Fujikura, K., Mitarai, S., 2014. Life history traits of Lepetodrilus nux in the Okinawa Trough, based upon gametogenesis, shell size, and genetic variability. Mar. Ecol. Prog. Ser. 505, 119–130. https://doi.org/10.3354/meps10779

Oksanen, J., Blanchet, F.G., Friendly, M., Kindt, R., Legendre, P., McGlinn, D., Minchin, P.R., O'Hara, R.B., Simpson, G.L., Solymos, P., Stevens, M.H.H., Szoecs, E., Wagner, H., 2019. vegan: Community Ecology Package.

Ondreas, H., Cannat, M., Fouquet, Y., Normand, A., Sarradin, P., Sarrazin, J., 2009. Recent volcanic events and the distribution of hydrothermal venting at the Lucky Strike hydrothermal field, Mid-Atlantic Ridge. Geochem. Geophys. Geosystems 10. https://doi.org/10.1029/2008gc002171

Orcutt, B.N., Bradley, J.A., Brazelton, W.J., Estes, E.R., Goordial, J.M., Huber, J.A., Jones, R.M., Mahmoudi, N., Marlow, J.J., Murdock, S., Pachiadaki, M., 2020. Impacts of deep-sea mining on microbial ecosystem services. Limnol. Oceanogr. n/a. https://doi.org/10.1002/lno.11403

Paine, R.T., 1966. Food Web Complexity and Species Diversity. Am. Nat. 100, 65–75.

Sancho, G., Fisher, C.R., Mills, S., Micheli, F., Johnson, G.A., Lenihan, H.S., Peterson, C.H., Mullineaux, L.S., 2005. Selective predation by the zoarcid fish Thermarces cerberus at hydrothermal vents. Deep Sea Res. Part Oceanogr. Res. Pap. 52, 837–844. https://doi.org/10.1016/j.dsr.2004.12.002

Sarradin, P.-M., Waeles, M., Bernagout, S., Le Gall, C., Sarrazin, J., Riso, R., 2009. Speciation of dissolved copper within an active hydrothermal edifice on the Lucky Strike vent field (MAR, 37°N). Sci. Total Environ. 407, 869–878. https://doi.org/10.1016/j.scitotenv.2008.09.056

Sarrazin, J., Cuvelier, D., Peton, L., Legendre, P., Sarradin, P.M., 2014. High-resolution dynamics of a deep-sea hydrothermal mussel assemblage monitored by the EMSO-Açores MoMAR observatory. Deep Sea Res. Part Oceanogr. Res. Pap. 90, 62–75. https://doi.org/10.1016/j.dsr.2014.04.004

Sarrazin, J., Levesque, C., Juniper, S., Tivey, M., 2002. Mosaic community dynamics on Juan de Fuca Ridge sulphide edifices: substratum, temperature and implications for trophic structure. CBM - Cahiers de Biologie Marine 43, 275–279.

Sarrazin, J., Juniper, S.K., Massoth, G., Legendre, P., 1999. Physical and chemical factors influencing species distributions on hydrothermal sulfide edifices of the Juan de Fuca Ridge, northeast Pacific. Mar. Ecol. Prog. Ser. 190, 89–112. https://doi.org/10.3354/meps190089

Sarrazin, J., Legendre, P., de Busserolles, F., Fabri, M.-C., Guilini, K., Ivanenko, V.N., Morineaux, M., Vanreusel, A., Sarradin, P.-M., 2015a. Biodiversity patterns, environmental drivers and indicator species on a high-temperature hydrothermal edifice, Mid-Atlantic Ridge. Deep Sea Res. Part II Top.

Stud. Oceanogr., Exploring New Frontiers in Deep-Sea Research: In Honor and Memory of Peter A. Rona 121, 177–192. https://doi.org/10.1016/j.dsr2.2015.04.013

Sarrazin, J., Portail, M., Legrand, E., Cathalot, C., Laes, A., Lahaye, N., Sarradin, P.M., Husson, B., 2020. Endogenous versus exogenous factors: What matters for vent mussel communities? Deep Sea Res. Part Oceanogr. Res. Pap. 103260. https://doi.org/10.1016/j.dsr.2020.103260

Sarrazin, J., V, R., Sk, J., Jr, D., 1997. Biological and geological dynamics over four years on a high-temperature sulfide structure at the Juan de Fuca Ridge hydrothermal observatory. Mar. Ecol. Prog. Ser. 153, 5–24. https://doi.org/10.3354/meps153005

Scheirer, D.S., Shank, T.M., Fornari, D.J., 2006. Temperature variations at diffuse and focused flow hydrothermal vent sites along the northern East Pacific Rise. Geochem. Geophys. Geosystems 7. https://doi.org/10.1029/2005GC001094

Sen, A., Becker, E.L., Podowski, E.L., Wickes, L.N., Ma, S., Mullaugh, K.M., Hourdez, S., Luther, G.W., Fisher, C.R., 2013. Distribution of mega fauna on sulfide edifices on the Eastern Lau Spreading Center and Valu Fa Ridge. Deep Sea Res. Part Oceanogr. Res. 72, 48–60. https://doi.org/10.1016/j.dsr.2012.11.003

Sen, A., Podowski, E.L., Becker, E.L., Shearer, E.A., Gartman, A., Yücel, M., Hourdez, S., Luther, G.W., III, Fisher, C.R., 2014. Community succession in hydrothermal vent habitats of the Eastern Lau Spreading Center and Valu Fa Ridge, Tonga. Limnol. Oceanogr. 59, 1510–1528. https://doi.org/10.4319/lo.2014.59.5.1510

Shank, T.M., Fornari, D.J., Von Damm, K.L., Lilley, M.D., Haymon, R.M., Lutz, R.A., 1998. Temporal and spatial patterns of biological community development at nascent deep-sea hydrothermal vents (9°50′N, East Pacific Rise). Deep Sea Res. Part II Top. Stud. Oceanogr. 45, 465–515. https://doi.org/10.1016/S0967-0645(97)00089-1

Sousa, W.P., 1985. Disturbance and patch dynamics on rocky intertidal shores. The ecology of natural disturbance and patch dynamics.

Spiess, F.N., Macdonald, K.C., Atwater, T., Ballard, R., Carranza, A., Cordoba, D., Cox, C., Garcia, V.M., Francheteau, J., Guerrero, J., Hawkins, J., Haymon, R., Hessler, R., Juteau, T., Kastner, M., Larson, R., Luyendyk, B., Macdougall, J.D., Miller, S., Normark, W., Orcutt, J., Rangin, C., 1980. East pacific rise: hot springs and geophysical experiments. Science 207, 1421–1433. https://doi.org/10.1126/science.207.4438.1421

Suzuki, K., Yoshida, K., Watanabe, H., Yamamoto, H., 2018. Mapping the resilience of chemosynthetic communities in hydrothermal vent fields. Sci. Rep. 8, 9364. https://doi.org/10.1038/s41598-018-27596-7

Tengberg, A., Hovdenes, J., Andersson, H.J., Brocandel, O., Diaz, R., Hebert, D., Arnerich, T., Huber, C., Körtzinger, A., Khripounoff, A., Rey, F., Rönning, C., Schimanski, J., Sommer, S., Stangelmayer, A., 2006. Evaluation of a lifetime-based optode to measure oxygen in aquatic systems. Limnology and Oceanography: Methods 4, 7–17. https://doi.org/10.4319/lom.2006.4.7

Tolstoy, M., Cowen, J.P., Baker, E.T., Fornari, D.J., Rubin, K.H., Shank, T.M., Waldhauser, F., Bohnenstiehl, D.R., Forsyth, D.W., Holmes, R.C., Love, B., Perfit, M.R., Weekly, R.T., Soule, S.A., Glazer, B., 2006. A Sea-Floor Spreading Event Captured by Seismometers. Science 314, 1920–1922. https://doi.org/10.1126/science.1133950

928 Tunnicliffe, V., 1991. The biology of hydrothermal vents : ecology and evolution. Biol. Hydrothermal
929 Vents Ecol. Evol. 29, 319–407.

930 Tunnicliffe, V., Embley, R.W., Holden, J.F., Butterfield, D.A., Massoth, G.J., Juniper, S.K., 1997. Biological
931 colonization of new hydrothermal vents following an eruption on Juan de Fuca Ridge. Deep Sea Res.
932 Part Oceanogr. Res. Pap. 44, 1627–1644. https://doi.org/10.1016/S0967-0637(97)00041-1

933 Van Audenhaege, L., Fariñas-Bermejo, A., Schultz, T., Lee Van Dover, C., 2019. An environmental
934 baseline for food webs at deep-sea hydrothermal vents in Manus Basin (Papua New Guinea). Deep Sea
935 Res. Part Oceanogr. Res. Pap. 148, 88–99. https://doi.org/10.1016/j.dsr.2019.04.018

936 Van Dover, C.L., 2007. The biological environment of polymetallic sulphides deposits, the potential
937 impact of exploration and mining on this environment, and data required to establish environmental
938 baselines in exploration areas. In: Polymetallic Sulphides and Cobalt-rich Ferromanganese Crusts
939 Deposits: Establishment of Environmental Baselines and an Associated Monitoring Programme during
940 Exploration. Proceedings of the International Seabed Authority's Workshop held in Kingston, Jamaica,
941 6e10 September 2004. Prepared by Offices of Resources and Environmental Monitoring (OREM), pp.
942 169e190. International Seabed Authority, Kingston, Jamaica: http://www.isa.org.jm/files/
943 documents/EN/Workshops/2004/Proceedings-ae.pdf. (accessed 13.06.13.).

944 Van Dover, C.L., 2011. Mining seafloor massive sulphides and biodiversity: what is at risk? ICES J. Mar.
945 Sci. 68, 341–348. https://doi.org/10.1093/icesjms/fsq086

946 Van Dover, C.L., 2010. Mining seafloor massive sulphides and biodiversity: what is at risk? ICES J. Mar.
947 Sci. 68, 341–348. https://doi.org/10.1093/icesjms/fsq086

948 Vuillemin, R., Le Roux, D., Dorval, P., Bucas, K., Sudreau, J.P., Hamon, M., Le Gall, C., Sarradin, P.M.,
949 2009. CHEMINI: A new in situ CHEmical MINIaturized analyzer. Deep Sea Res. Part Oceanogr. Res. Pap.
950 56, 1391–1399. https://doi.org/10.1016/j.dsr.2009.02.002

951 Washburn, T.W., Turner, P.J., Durden, J.M., Jones, D.O.B., Weaver, P., Van Dover, C.L., 2019. Ecological
952 risk assessment for deep-sea mining. Ocean Coast. Manag. 176, 24–39.
953 https://doi.org/10.1016/j.ocecoaman.2019.04.014

954 Zajac, R.N., Whitlatch, R.B., Thrush, S.F., 1998. Recolonization and succession in soft-sediment infaunal
955 communities: the spatial scale of controlling factors. Hydrobiologia 375, 227–240.
956 https://doi.org/10.1023/A:1017032200173

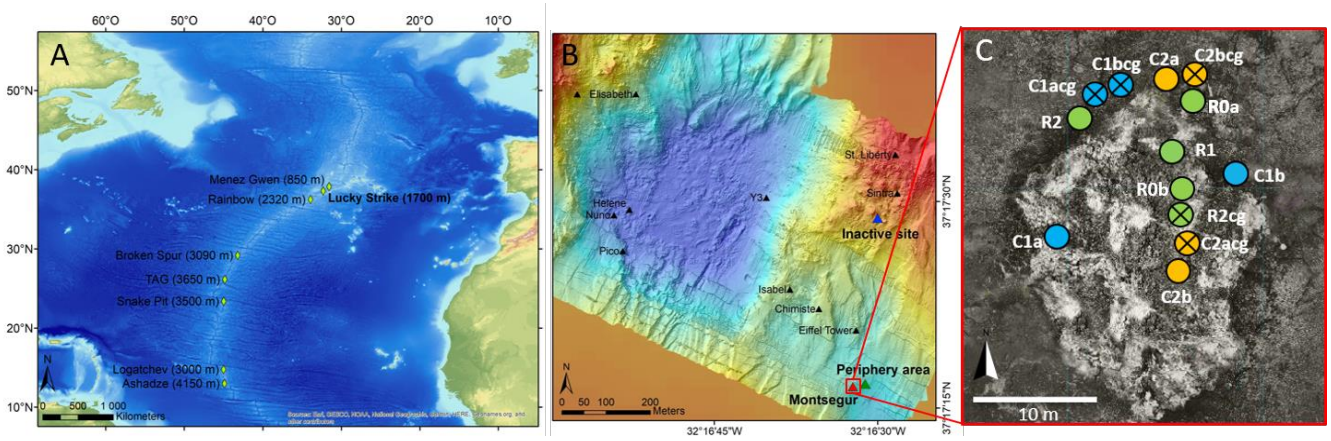

Figure 1. A. Location of the Lucky Strike (LS) vent field along the Mid-Atlantic Ridge. **B**. Bathymetric chart of LS and location of the Montségur edifice **C**. Position of the experimental and reference quadrats on and around the Montségur edifice. Green circles represent the reference quadrats, blue circles represent the experimental quadrats used to study the recolonisation 1 year after the disturbance, and orange circles represent the experimental quadrats used to study the recolonisation 2 years after the disturbance. Crossed off circles represent "caged" quadrats while empty circles represent quadrats without a cage.

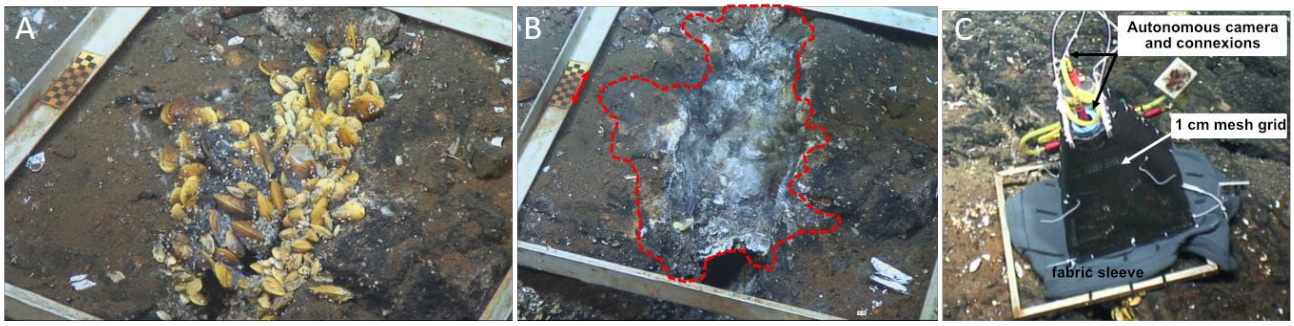

Figure 2. The C1a-cg experimental quadrat in 2017, (**A**) before faunal clearance (baseline community) and ; (**B**) after the induced disturbance. Red arrow highlights the check-board used to calibrate imagery analysis and estimate the sampling surface area (red dotted line). (**C**) The C1bcg "caged" experimental quadrat used to exclude large mobile predators. A 1 cm mesh grid was adjusted on the pyramidal structure on top of the quadrat (in black on the picture) and a grey fabric sleeve was attached to the edge of the caged quadrat to avoid colonisation of crawlers. A camera was deployed at the top of the pyramidal structure and connected to a battery on the side (yellow cables).

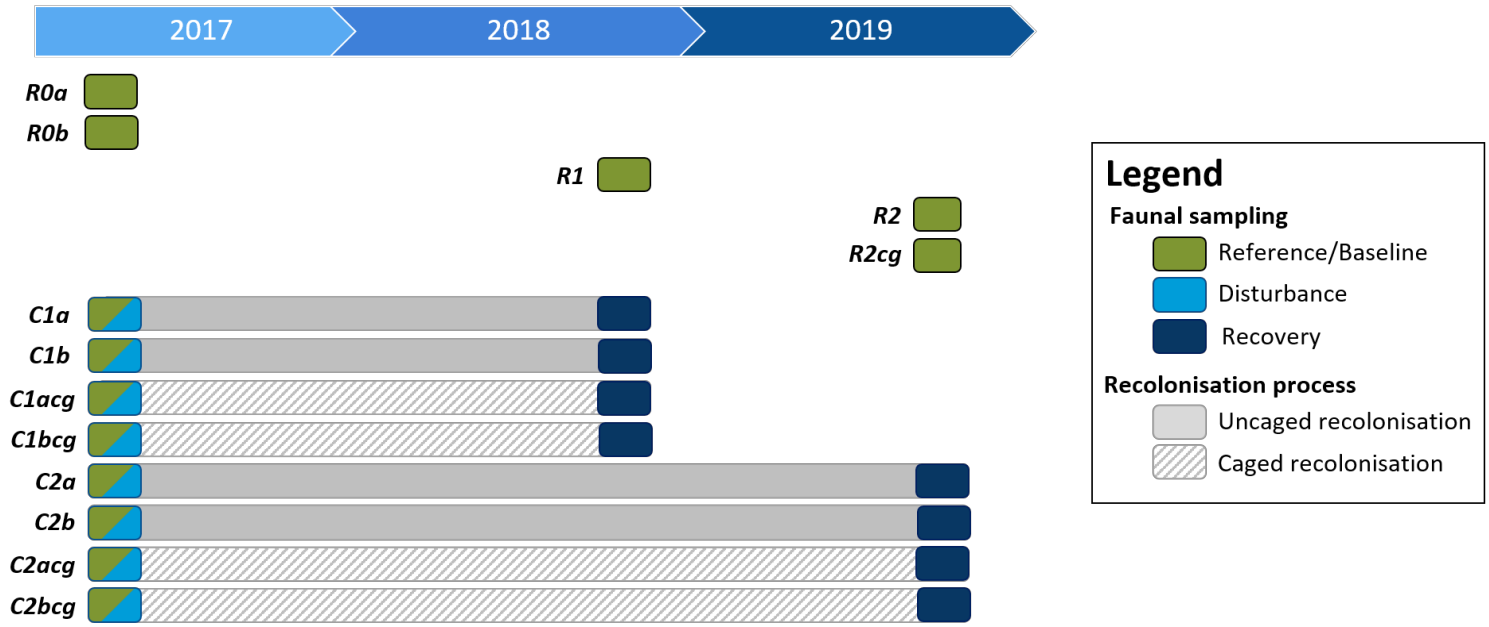

Figure 3. Experimental design of the disturbance experiment deployed between 2017 and 2019 on the Montségur edifice, Lucky Strike vent field (Mid-Atlantic Ridge). Small rectangles represent faunal sampling and their color indicates the nature of the operation: green, sampling of baseline communities; light blue, induction of disturbance by clearing faunal assemblages; dark blue, sampling after recolonisation to evaluate the recovery. Grey segments represent the recolonisation period studied for each quadrat. Hatched segments indicate the presence of caged during the recolonisation period.

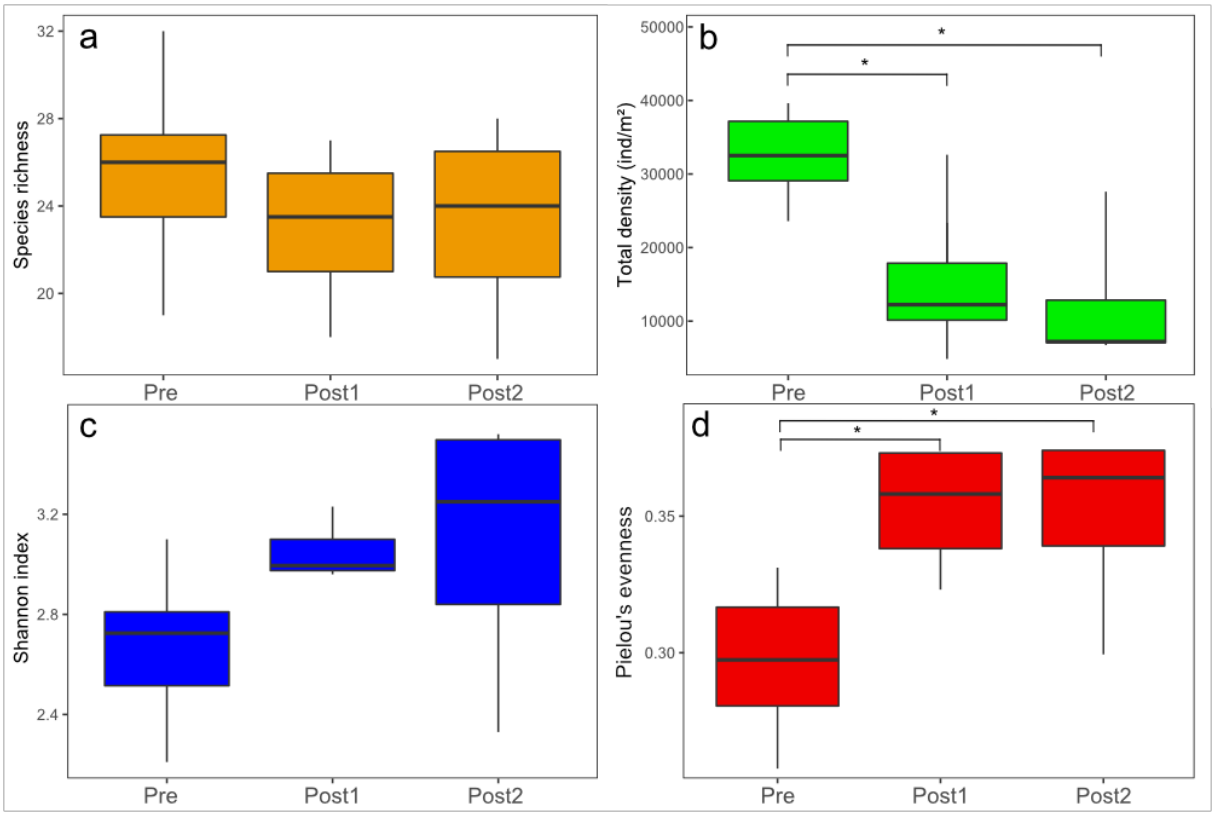

Figure 4. Species richness (**a**), total density (**b**), Shannon index (**c**) and Pielou's evenness index (**d**) of macrofaunal communities on the baseline communities and during the recolonisation process on the active Montségur edifice. Pre: assemblages sampled before the disturbance; Post1: assemblages sampled 1 year after the disturbance; Post2: assemblages sampled 2 years after the disturbance. Significance of Kruskall-Wallis multisample tests and post-hoc Dunn's tests are represented on the top of the boxplots.

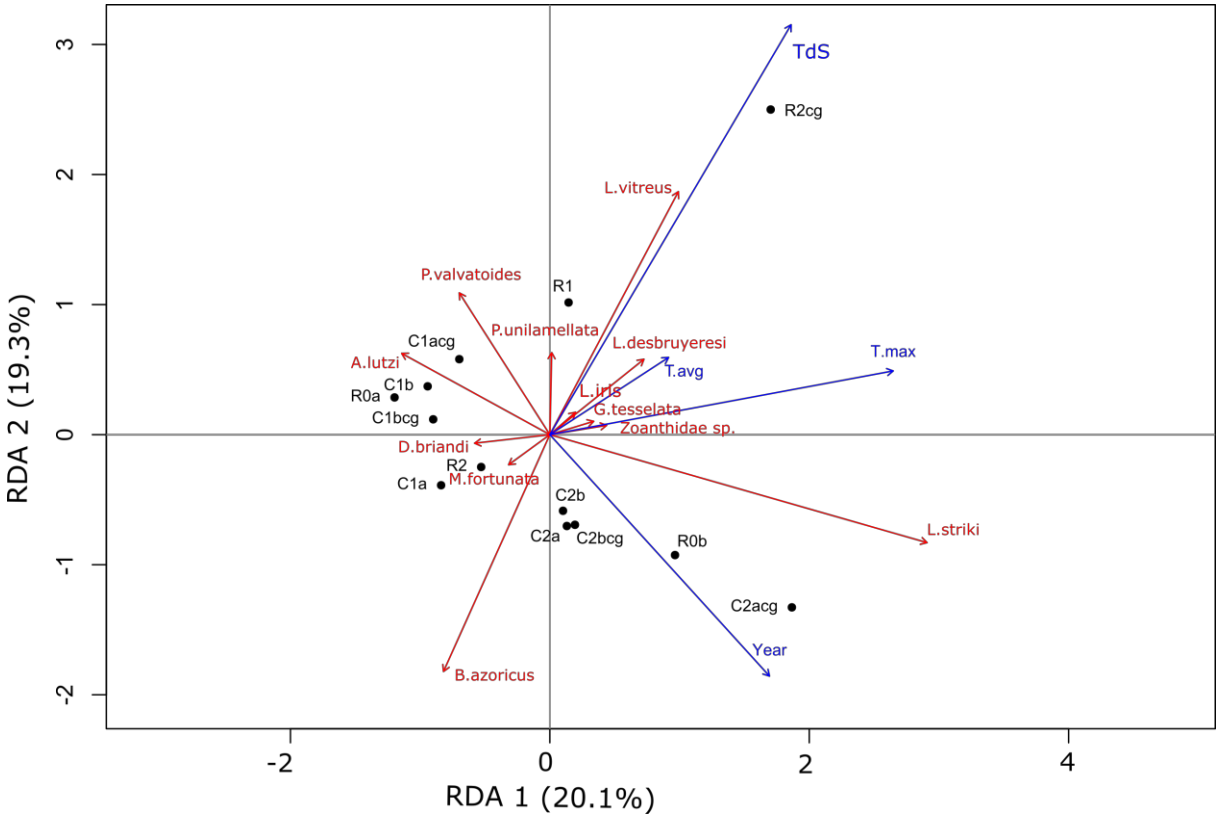

Figure 5. Canonical redundancy analysis (RDA, scaling 2) of Hellinger-transformed macrofaunal densities observed in the baseline community of the Montségur active edifice at the Lucky Strike vent field (Mid-Atlantic Ridge). The first canonical axis represents 20.1 % of the total variance in macrofaunal densities while the second axis represents 19.3% (adj R^2 = 25.1%, p = 0.004). The first axis is significant (p = 0.05). Only species that accounted for more than 50% of cumulative inertia on the two first axes are represented.

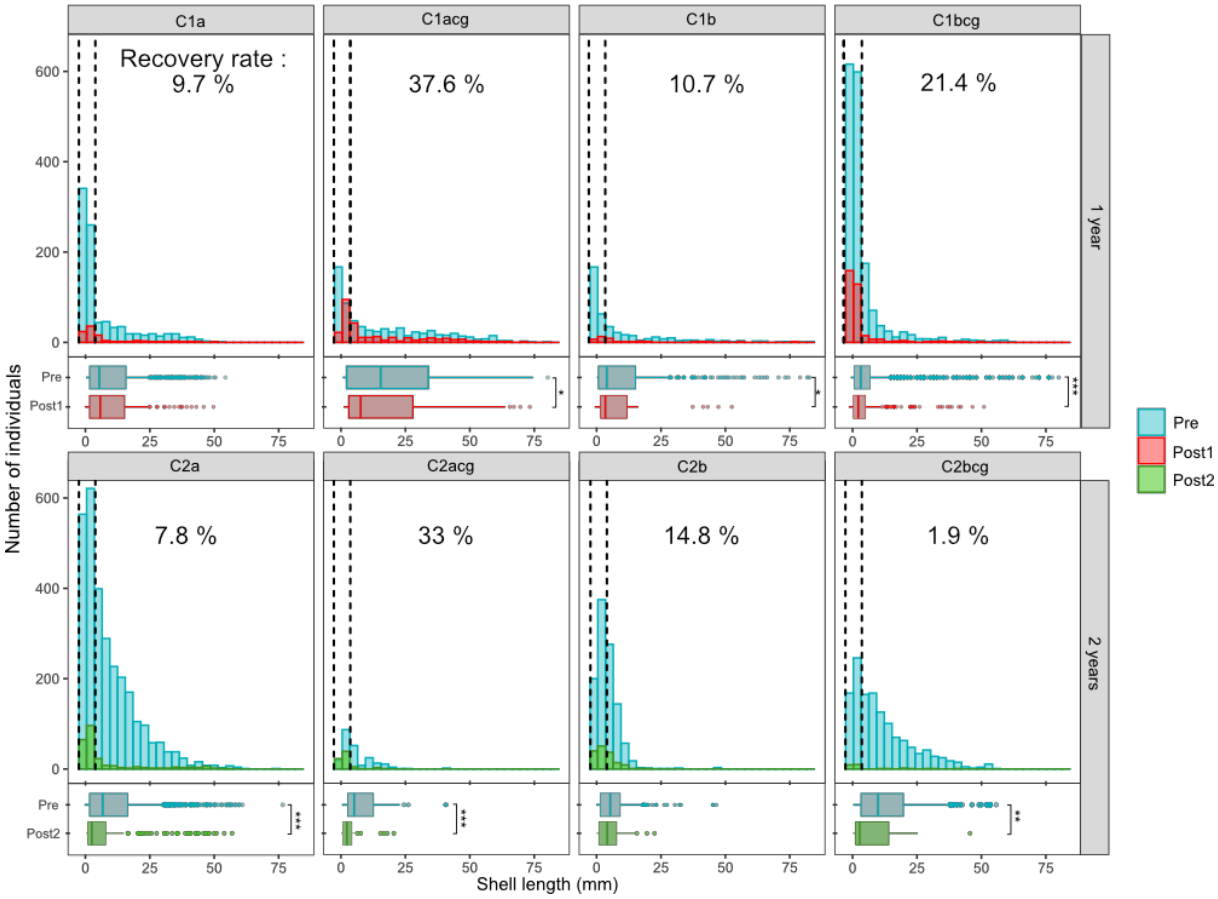

Figure 6. Histograms and boxplots of size frequency distribution of *Bathymodiolus azoricus* for each quadrat sampled at the Montségur edifice at the Lucky Strike vent field (Mid-Atlantic Ridge) including the pre-disturbed community (blue) and the communities one (red) and 2 (green) years after disturbance. Wilcoxon-Mann-Whitney tests were performed to identify differences in mean individual size between the baseline and post-disturbance communities. Asterisks indicate significant differences in mean shell length (*p-value<0.05; ** p-value <0.01; *** p-value <0.001). The interval between dotted lines represents the range of size at recruitment. The percentages represent the proportion of *B. azoricus* density which recovered in comparison of the pre-disturbed value in each quadrat.

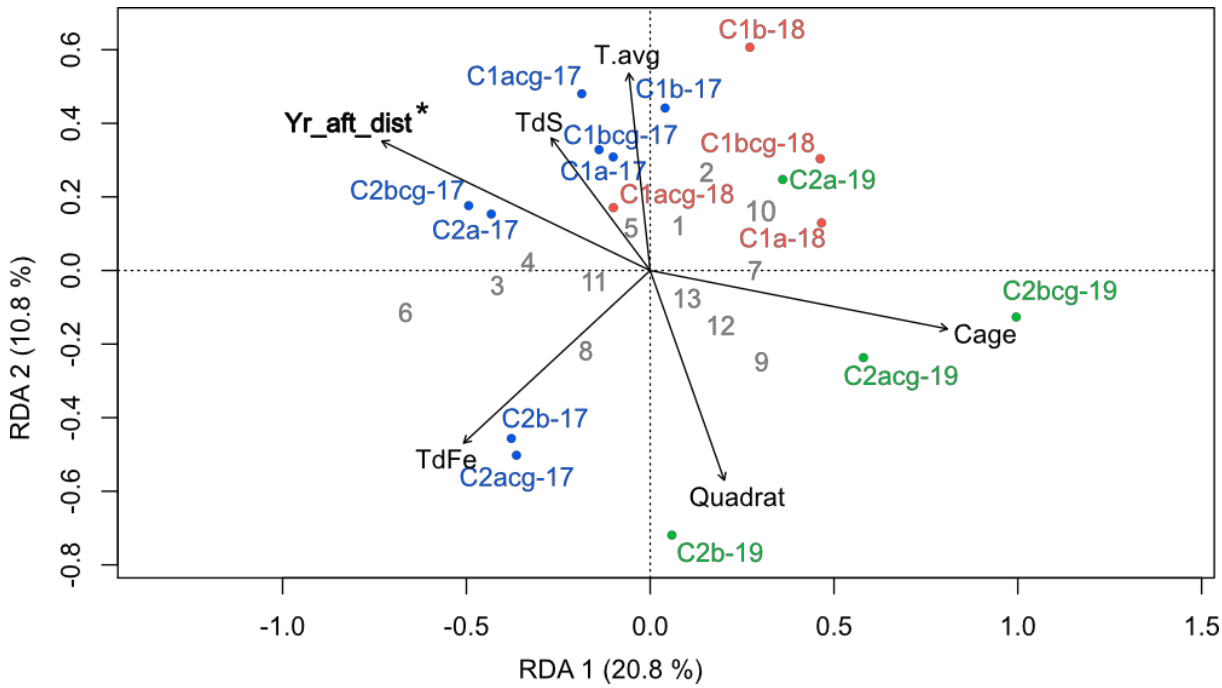

Figure 7. Canonical redundancy analysis (RDA, scaling 2) of Hellinger-transformed macrofaunal densities observed in the different assemblages during the recolonization process at the Montségur active edifice (Lucky Strike vent field, Mid-Atlantic Ridge). The first canonical axis represents 20.8% of the total variance in macrofaunal densities while the second axis represents 10.8% (with an adjusted R^2 of 20.5%). The RDA and the first axis are significant (p-values =0.006 and 0.023, respectively). Only species showing good fit with the first two canonical axes are represented. Colors refer to the time after disturbance: baseline communities (blue); 1 year after disturbance (red); two years after disturbance (green). Explanatory variables: Years after disturbance (*Yr_aft_dist*), average temperature measured before sampling (*T.avg*), mean concentration of total dissolved sulphides (*TdS*), mean concentration of total dissolved iron (*TdFe*), if quadrats are caged or uncaged (*Cage*), identification of quadrats to test the dependence of the same location over the time of the experiment (*Quadrat*). Response variables, each species is designated by a number: 1 – *Amphisamytha lutzi*; 2 – *Aphotopontius sp.*; 3 – *Bathymodiolus azoricus*; 4 – *Branchipolynoe seepensis*; 5 – *Lepetodrilus atlanticus*; 6 – *Lirapex costellata*; 7 – *Laeviphitus desbruyeresi*; 8 – *Luckia striki*; 9 – *Lurifax vitreus*; 10 – *Oncholaimus dyvae*; 11 – *Paralepetopsis ferrugivora*; 12 – *Protolira valvatoides*; 13 – *Xylodiscula analoga*.

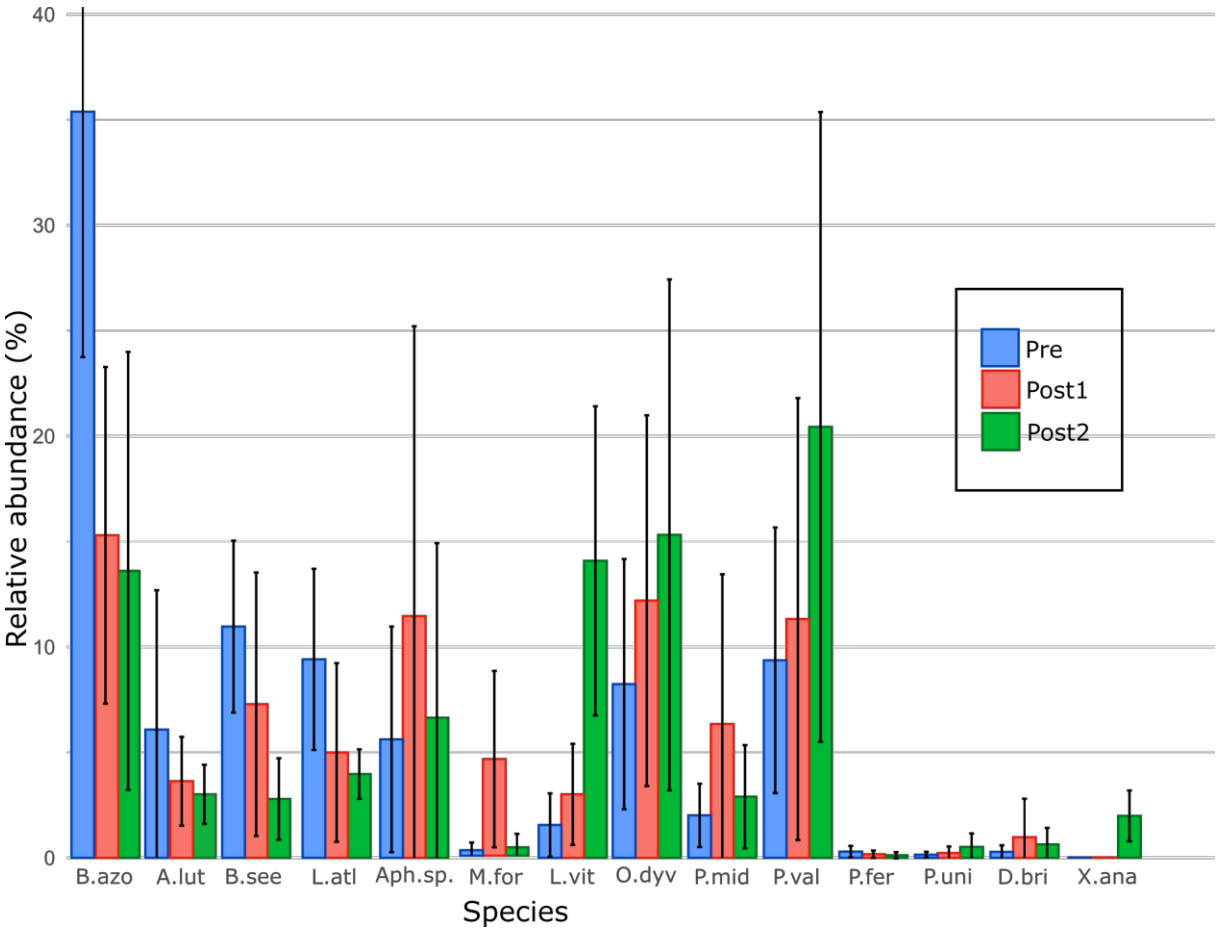

Figure 8. Mean and standard deviations of densities for the most abundant species among the experimental quadrats on the active Montségur edifice before the disturbance (Pre) and one/two years after the disturbance (Post1 and Post2). Species acronyms: B.azo – *Bathymodiolus azoricus*, A.lut – *Amphisamytha lutzi*; B.see – *Branchipolynoe seepensis*; L.atl – *Lepetodrilus atlanticus*; Aph.sp. – *Aphotopontius sp.*; M.for – *Mirocaris fortunata*; L.vit – *Lurifax vitreus*; O.dyv – *Oncholaimus dyvae*; P.mid – *Pseudorimula midatlantica*; P.val – *Protolira valvatoides*; P.uni – *Prionospio unilamellata*; D.bri – *Divia briandi*; X.ana – *Xylodiscula analoga*.

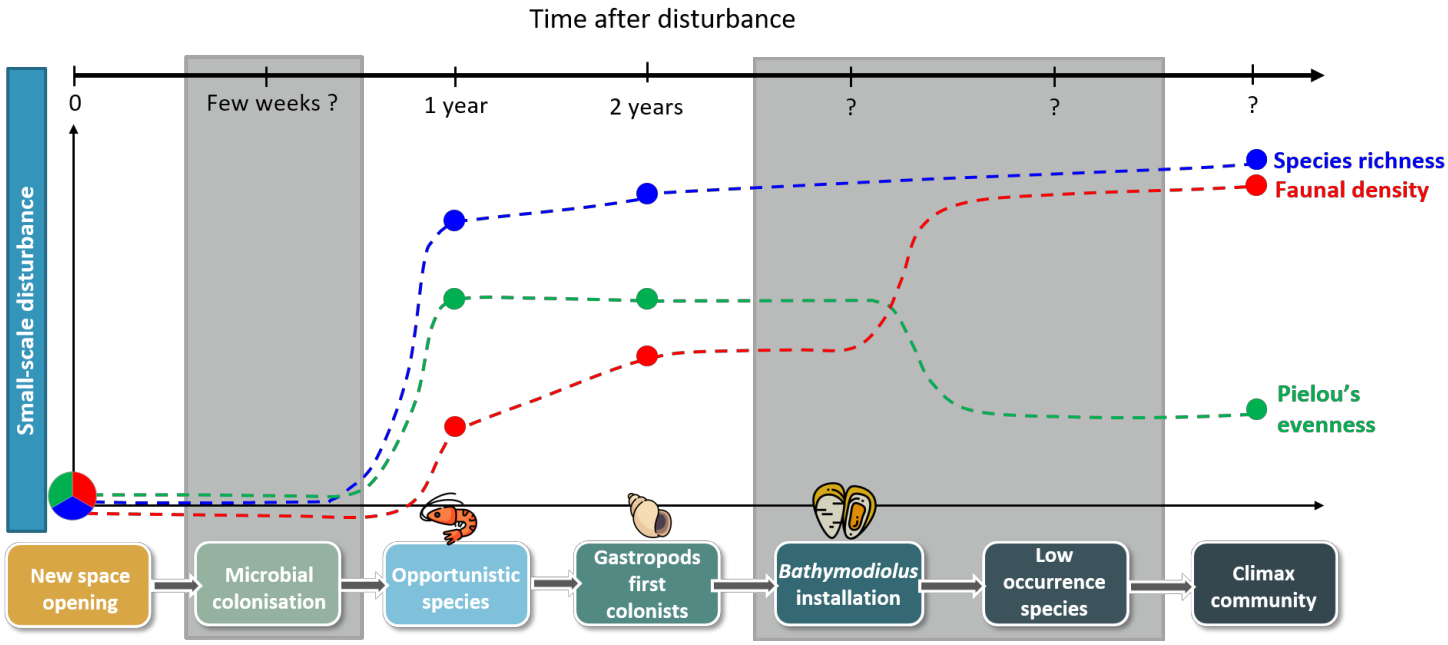

Figure 9. Conceptual model of colonisation and ecological succession until climax after a small-scale disturbance on the Lucky Strike vent assemblages (MAR). Evolution of species richness, faunal densities and Pielou's evenness index during the recovery process, based on the main results of our disturbance experiment (solid dots) and inferred from the literature (grey boxes).

Table 1. Environmental conditions on the baseline communities of the different quadrats deployed on the Montségur edifice (Lucky Strike vent field, Mid-Atlantic Ridge). Temperature: average: T.avg., standard deviation: T.std. maximum: T.max and minimum: T.min. from iButtons^{TM}. Oxygen (O_2). Total dissolved sulphide (TdS) and Total dissolved iron (TdFe) measured with the *in situ* analysers CHEMINI. Methane (CH_4) and pH were measured through quantitative analyses from samples collected with the PEPITO water sampler (Sarradin et al. 2009). Highest values are highlighted in bold and lowest values in grey.

Quadrat	T.avg	T.std	T.min	T.max	O_2 (µM)	TdS (µM)	TdFe (µM)	CH_4 (µM)	pH
					Mean ± SD				
Montségur									
R0a	*5.2*	*0.2*	*4.6*	*6.1*	*208.2 ± 0.1*	2.7 ± 0.2	0.2 ± 0.1	0.4	**7.8**
R0b	6.9	0.8	5.1	11.5	207.2 ± 0.4	3.1 ± 1.0	1.1 ± 0.3	0.5	7.6
R1	**9.5**	**2.7**	**6.1**	**22.1**	206.1 ± 1.1	2.3 ± 0.2	**2.2 ± 0.2**	**2.1**	7.2
R2	5.5	0.4	5.1	11.4	206.9 ± 1.3	3.2 ± 2.7	0.2 ± 0.1	0.9	7.5
R2cg	5.3	0.2	4.6	7.1	205.6 ± 0.6	0.9 ± 0.2	0.6 ± 1.1	*0.2*	7.9
C1a	6.1	0.3	5.1	7.1	207.4 ± 0.1	3.2 ± 0.8	0.2 ± 0.1	0.7	7.6
C1acg	5.8	1.2	4.6	12.1	204.3 ± 1.5	3.9 ± 2.6	0.3 ± 0.1	**2.1**	7.2
C1b	6.4	0.4	4.6	10.6	206.2 ± 1	**10.8 ± 14.7**	0.3 ± 0.3	1.1	7.4
C1bcg	5.7	0.42	4.6	8.1	207.9 ± 0.4	2.5 ± 0.6	0.2 ± 0.1	0.8	7.7
C2a	**7.6**	**1.12**	**6.1**	**16.1**	203.8 ± 2.1	**23.2 ± 26.3**	1.1 ± 0.3	**15.2**	6.1
C2acg	6.3	0.5	5	8.6	207.4 ± 0.8	1.3 ± 0.1	0.9 ± 0.8	0.7	7.7
C2b	5.3	0.2	5	*6.1*	205.2 ± 0.5	3.8 ± 3.8	0.9 ± 0.4	0.4	7.8
C2bcg	5.3	0.3	4.6	6.6	206.6 ± 0.3	5.6 ± 1.2	0.2 ± 0.1	**2.0**	7.2

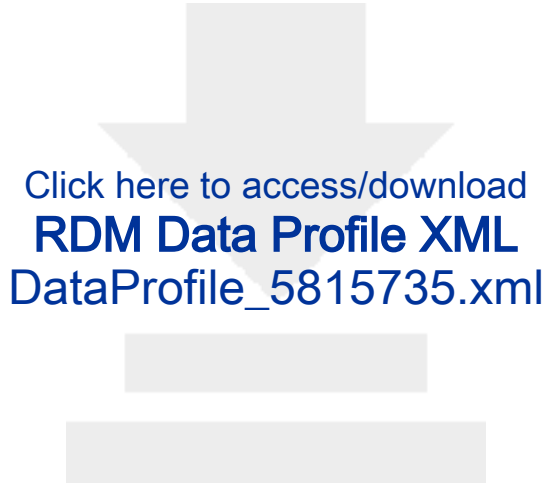

Declaration of interest

The authors declare no competing interests.

Author Statement

JM, MM and JS conceived the ideas and designed the methodology. JM, MM, JS, ALH and CC collected the samples on board during oceanographic cruises. JM, MM, JS, ALH, CC, JPD and SH processed and analysed the data. JM and RL did the statistical analyses. JM, MM, ERL and JS discussed and interpreted the results. JM wrote the first draft of the manuscript and all authors commented on previous versions of the manuscript. All authors read and approved the final manuscript.